3) 生尾博子、中尾篤人、三宅健介、奥村　康、小川秀興: MD-2 is required for the full-responsiveness of mast cells to LPS but not to PGN. 第 33 回日本免疫学会 2003 年 12 月

4) 生尾博子、原むつ子、フランソワ　ニヨンサバ、奥村　康、小川秀興: ファイブロネクチンフラグメントによる TLR4 を介したマスト細胞の活性化. 第 54 回日本アレルギー学会、2004 年 11 月

5) フランソワ　ニヨンサバ、生尾博子、原むつ子、長岡　功、奥村　康、小川秀興: 上皮組織が産生する殺菌ペプチド・β-defensin と LL-37 のケラチノサイトに及ぼす影響、第 54 回日本アレルギー学会、2004 年 11 月

6) Niyonsaba Francois、生尾博子、原むつ子、奥村　康、小川秀興: Murine mast cells express functional Toll-like receptor 3 that activates nuclear factor kappa B and MAP kinase ERK and p38、第 34 回日本免疫学会、2004 年 11 月

7) 生尾博子、原むつ子、フランソワ　ニヨンサバ、奥村　康、小川秀興: ファイブロネクチンフラグメントによる TLR4 を介したマスト細胞の活性化、第 34 回日本免疫学会、2004 年 11 月

8) Chen Xuejun, Niyonsaba Francois、生尾博子、長岡　功、奥村　康、小川秀興: Synergistic effect of human antimirobial peptides and lysozyme on Staphylococcus aureus and Esherichia coli. 第 34 回日本免疫学会、2004 年 12

9) Sampnthanrak Pichai, Niyonsaba Francois、生尾博子、奥村　康、小川秀興: The effect of antibacterial peptide human beta-defensin-2 on interleukin-18 secretion by keratinocyte. 第 34 回日本免疫学会、2004 年 12 月

H. 知的財産権の出願・登録状況：該当なし

研究成果の刊行に関する一覧表

書籍

著者氏名	論文タイトル名	書籍全体の編集者名	書　籍　名	出版社名	出版地	出版年	ページ

雑誌

発表者氏名	論文タイトル名	発表誌名	巻号	ページ	出版年
Sampanthanarak P, Niyonsaba F, Ushio H, Nagaoka I, Ikeda S, Okumura K, Ogawa H.	The effect of antibacterial peptide human beta-defensin-2 on interleukin-18 secretion by keratinocytes.	J Dermatol Sci	37(3)	188-91	2005
Ito T, Nishiyama C, Nishiyama M, Matsuda H, Maeda K, Akizawa Y, Tsuboi R, Okumura K,and Ogawa H.	Mast cells acquire monocyte-specific gene expression and monocyte-like morphology by overproduction of PU.1.	J Immunol	174	376–383	2005
Hasegawa T, Nakao A, Sumiyoshi K, Tsuchihashi H, Ogawa H.	SB-431542 inhibits TGF-β-induced contraction of collagen gel by normal and keloid fibroblasts.	J Dermatol Sci	in press	in press	2005
Okamoto A, Kawamura T, Kanbe K, Kanamaru Y, Ogawa H, Okumura K, Nakao A.	Suppression of serum IgE response and systemic anaphylaxis in a food allergy model by orally administered high-dose TGF-β_	Int Immunol	in press	in press	2005
Kanamaru Y, Sumiyoshi K, Ushio H, Ogawa H, Okumura K, Nakao A.	Smad3 deficiency in mast cells provides efficient host protection against acute septic peritonitis.	J Immunol	in press	in press	2005
Inazaki K, Kanamaru Y, Kojima Y, Sueyoshi N, Okumura K, Kaneko K, Yamashiro Y, Ogawa H, Nakao A.	Smad3 deficiency attenuates renal fibrosis, inflammation, and apoptosis after unilateral ureteral obstruction.	Kidney Int	66	597-604	2004

発表者氏名	論文タイトル名	発表誌名	巻号	ページ	出版年
Jin L, Nakao A, Nakayama M, Yamaguchi N, Kojima Y, Nakano N, Tsuboi R, Okumura K, Yagita H, Ogawa H.	Induction of RANTES by TWEAK/Fn14 interaction in human keratinocytes.	J Invest Dermatol	122	1175-1179	2004
Sumiyoshi K, Nakao A, Setoguchi Y, Okumura K, Ogawa H.	Exogenous Smad3 accelerates wound healing in a rabbit dermal ulcer model.	J Invest Dermatol	123	229-236	2004
Ito K, Hanazawa T, Tomita K, Barnes PJ, Adcock IM.	Oxidative stress reduces histone deacetylase 2 activity and enhances IL-8 gene expression: role of tyrosine nitration..	Biochem Biophys Res Commun	27;315(1)	240-5	2004
Xu H, Okamoto A, Ichikawa J, Ando T, Tasaka K, Masuyama K, Ogawa H, Yagita H, Okumura K, Nakao A.	TWEAK/Fn14 interaction stimulates human bronchial epithelial cells to produce IL-8 and GM-CSF.	Biochem Biophys Res Commun	318	422-427	2004
Ushio H, Nakao A, Supajatura V, Miyake K, Okumura K, Ogawa H.	MD-2 is required for the full responsiveness of mast cells to LPS but not to PGN.	Biochem Biophys Res Commun	323	491-498	2004
Komine-Kobayashi M, Chou N, Mochizuki H, Nakao A, Mizuno Y, Urabe T.	Dual role of Fcγ receptor in transient focal cerebral ischemia in mice.	Stroke	35	958-963	2004
Prapars M, Nakao A, Nakano H, Jin L, Ogawa H.	Expression of phosphorylated Smad2 in normal human epidermis.	J Dermatol Sci	34	54-55	2004
Sugita T, Tajima M, Amaya M, Tsuboi R, Nishikawa A.	Genotype analysis of Malassezia restricta as the major cutaneous flora in patients with Atopic dermatitis and healthy subjects.	Microbiol Immunol	48	755-759	2004
Sugita T, Tajima M, Takashima M, Tsuboi R, Nishikawa A.	A new Yeast, Malassezia yamatoensis, Isolated from a patient with seborrheic dermatitis, and its distribution in patients and healthy subjects.	Microbiol Immunol	48	579-583	2004
Furuse Y, Hashimoto N, Maekawa M, Toyama Y, Nakao A, Iwamoto I, Sakurai K, Suzuki Y, Yagui K, Yuasa S, Toshimori K, Saito Y	Activation of the Smad pathway in glomeruli from a spontaneously diabetic rat model, OLETF rats	Nephron Exp Nephrol	98	100-108	2004

発表者氏名	論文タイトル名	発表誌名	巻号	ページ	出版年
Kawashima M, Hayashi N, Igarashi A, Kitahara H, Maeguchi M, Mizuno A, Murata Y, Nogita T, Toda K, Tsuboi R, Ueki R, Yamada M, Yamazaki M, Matsuda T, Natsumeda Y, Takahashi K, Harada S.	Finasteride in the treatment of Japanese men with male pattern hair loss.	Eur J Dermatol	14	247-254	2004

Journal of Dermatological Science (2005) 37, 188–191

ELSEVIER

Journal of Dermatological SCIENCE

www.intl.elsevierhealth.com/journals/jods

LETTER TO THE EDITOR

The effect of antibacterial peptide human β-defensin-2 on interleukin-18 secretion by keratinocytes

KEYWORDS
Keratinocyte;
Human antibacterial peptide;
β-Defensin;
Interleukin-18

A large number of antimicrobial peptides have been identified in humans, and among them human β-defensins (hBD), mainly produced by epithelium, have been well characterized. These peptides exhibit their killing activities against bacteria, fungi and certain viruses [1]. Among the hBD, hBD-2 that was originally isolated from psoriatic skin, is the most investigated human antibacterial peptide. In the skin, hBD-2 is produced by keratinocytes, the key cells involved in the cutaneous immunological network and the pathological changes of several skin diseases by producing abundant cytokines including interleukin (IL)-18. hBD-2 plays a crucial role in host defense under infectious and inflammatory conditions, and its expression increases in certain skin diseases such as psoriasis and atopic dermatitis (AD) [1]. Besides its bactericidal properties, we have recently reported that hBD-2 also activates mast cells and neutrophils [2,3].

IL-18, an interferon-γ inducer, is a pro-inflammatory cytokine generated by skin cells such as keratinocytes, macrophages, dendritic and Langerhans cells. IL-18 was originally considered as a Th1 cytokine acting through its ability to induce IFN-γ production, and its expression is highly enhanced in psoriasis [4]. However, recent studies have indicated a more complicated pleiotropic role for IL-18 than simply induction of IFN-γ production, and IL-18 was reported to induce the production of IgE and Th2 cytokines [4]. IL-18 was also recently found to be associated with the pathogenesis and severity of atopic dermatitis [5].

Since hBD-2 and IL-18 are generated by keratinocytes, and because they are both involved in psoriasis and atopic dermatitis, we hypothesized that they could interact with keratinocytes. Thus, the goal of this study was to investigate the interaction between keratinocytes, hBD-2 and IL-18 by evaluating the effect of hBD-2 on IL-18 secretion by keratinocytes.

Immortalized human keratinocyte cell line, HaCaT were grown in Dulbecco's modified Eagle's medium supplemented with 10% FBS and antibiotics, and were passaged or stimulated at 60–70% subconfluence. Cells were stimulated with hBD-2 (Peptide Institute, Osaka, Japan), and the concentration of IL-18 in the culture supernatants was measured by ELISA (Medical and Biological Laboratories, Nagoya, Japan) according to the manufacturer's instructions. In some experiments, to investigate the role of caspase-1 in IL-18 secretion, cells were incubated with the caspase-1 inhibitor (Ac-YVKD-CHO, Peptide Institute) before stimulation with hBD-2. The caspase-1 enzymatic activity was determined by using a caspase-1 colorimetric assay kit (Research and Development Systems, Minneapolis, MN). The IL-18 mRNA expression was analyzed by RT-PCR and the expression of pro-IL-18 protein was determined by Western blot analysis. The statistical analysis was performed using Student's t-test, and $p < 0.05$ was considered to be significant. The results are shown as mean ± standard deviation (S.D.).

As can be seen on Fig. 1A, the incubation of HaCat with 10 μg/ml of hBD-2 for 1–48 h resulted in significant IL-18 secretion at 1, 3 and 6 h ($p < 0.05$), before decreasing gradually. Furthermore, the secretion of IL-18 induced by hBD-2 was found to be dose-dependent as shown on Fig. 1B. The contact sensitizer dinitrochlorobenzene (DNCB) was used as a positive control [6]. In contrast, 1–20 μg/ml hBD-1, hBD-3 and human cathelicidin LL-37, an antimicrobial peptide also expressed in keratinocytes during inflammation, could not induce IL-18 secretion

doi:10.1016/j.jdermsci.2004.12.019

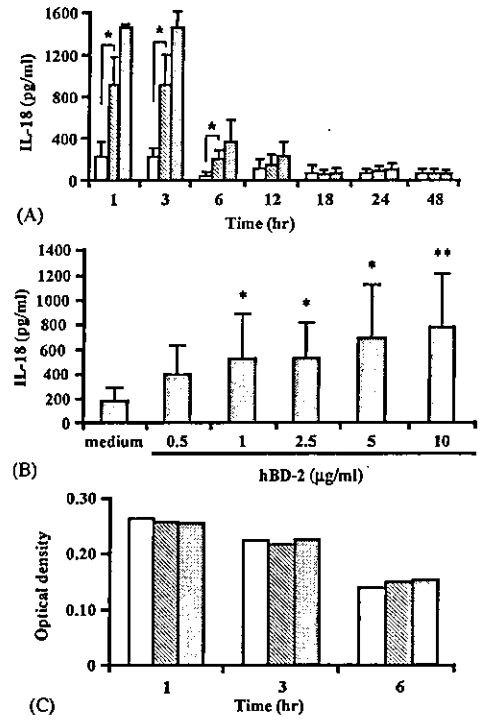

Fig. 1 Effects of hBD-2 on IL-18 secretion and caspase-1 enzymatic activity. (A) HaCaT cells were stimulated with 10 μg/ml hBD-2 (hatched bars) or 0.001% DNCB (closed bars) for 1 to 48 h, and the concentration of IL-18 in the supernatants was determined by ELISA. Values are compared between stimulated and non-stimulated cells (open bars). $^{*}p < 0.05$. Each bar represents the mean ± S.D. of five separate experiments. (B) Furthermore, the dose-dependent experiment was performed by incubating cells with increasing doses of hBD-2 (0.5–10 μg/ml), and the amounts of IL-18 secretion in the supernatants were determined by ELISA. Values are compared between stimulated and non-stimulated cells (medium). $^{*}p < 0.05$, $^{**}p < 0.01$. Each bar represents the mean ± S.D. of five separate experiments. (C) The caspase-1 enzymatic activity assay was performed using caspase-1 colorimetric assay kit according to the manufacturer's instructions. Non-stimulated cells (open bars) or cells stimulated with hBD-2 (hatched bars) or 0.001% DNCB (closed bars) at indicated period were trypsinised, and 2×10^6 cells were lysed in 50 μl of cold lysis buffer. The cell lysate was incubated on ice for 10 min, centrifuged at 10,000 × *g* for 1 min, and then the supernatant was collected. A volume of 50 μl cell lysate was added to 2.5 mM DTT and 50 μl of caspase reaction buffer. Each sample was added with 40 μM caspase-1 substrate WEHD-pNA followed by a 2 h-incubation at 37 °C. The enzymatic activity of caspase-1 was monitored on a microplate reader using 405 nm wavelength. The data normalized to the negative control are shown as optical density.

by HaCat at 1–48 h-incubation period (unpublished data).

As caspase-1 is required for cleavage of pro-IL-18 leading to the generation of mature IL-18, we next investigated the molecular mechanism underlying hBD-2-induced IL-18 secretion by performing the caspase-1 colorimetric assay, using specific substrate WEHD-pNA. The results revealed that hBD-2 could not increase the caspase-1 activity (Fig. 1C). To determine the role of caspase-1 in hBD-2-induced IL-18 secretion, cells were further treated with Ac-YVKD-CHO for 1 h before stimulation with hBD-2, and secreted IL-18 was analyzed by ELISA. As expected, Ac-YVKD-CHO could not suppress hBD-2-induced IL-18 secretion (data not shown). In addition, since caspase-1 is also responsible for the cleavage of pro-IL-1β to generate a functional mature IL-1β, we investigated whether hBD-2 could stimulate keratinocytes to generate IL-1β. However, hBD-2 could not induce IL-1β production (data not shown). Thus, one can suggest that hBD-2-induced IL-18 secretion by keratinocytes is unlikely mediated by caspase-1. Nakano et al. [7] have also reported that caspase-1 inhibitor could not inhibit IL-18 secretion from SpA-stimulated mouse keratinocytes. The same author has also shown that caspase-1 was not involved in IL-18 secretion by keratinocytes since caspase-1-deficient keratinocytes could secrete similar amounts of IL-18 as wild type keratinocytes. Up to date, the role of caspase-1 in keratinocytes is not well understood. Although caspase-1 has been demonstrated in human keratinocytes, it appears to exist in the unprocessed, biologically inactive form [8].

We next examined the effects of hBD-2 on the expression of IL-18 mRNA. As shown in Fig. 2A, IL-18 mRNA was constitutively expressed in keratinocytes, but its expression could not be increased upon the stimulation with hBD-2 at any incubation time period. This observation was consistent with a previous study showing that SpA, DNCB and pro-inflammatory mediators PMA and LPS induce IL-18 secretion by keratinocytes, but are unable to increase IL-18 mRNA expression [6,7]. It has been proposed that the inability to induce IL-18 mRNA in human keratinocytes may be partially due to the fact that the IL-18 gene possesses at least two promoters, one of which is constitutive in nature [9]. It seems that the inducible IL-18 promoter is inactive in human keratinocytes.

Furthermore, to elucidate whether hBD-2 may increase the expression of pro-IL-18 protein, cells were stimulated with hBD-2 and lysates were subjected to Western blot analysis. We detected a signal corresponding to the unprocessed form of IL-18 (24 kDa), and its expression level was not significantly changed following the stimulation with

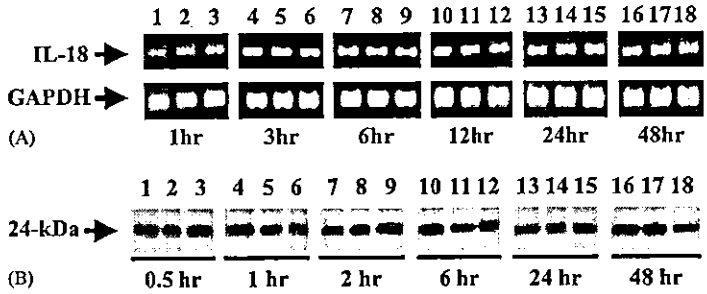

Fig. 2 mRNA expression of IL-18 and protein expression of pro-IL-18. (A) Total RNA (3 μg) isolated from non-stimulated or stimulated cells for indicated time period was analyzed for expression of IL-18 mRNA by RT-PCR. The primers used were: IL-18 (836 bp), sense primer AGGAATAAAGATGGCTGCTGAAC, antisense primer, GCTCACCACAACCTCTACCTCC; GAPDH (447 bp), sense primer ACCACAGTCCATGCCATCAC, antisense primer TCCACCACCCTGTTGCTGTA. The PCR amplification was used for 20 cycles (1 min at 95 °C, 1 min at 60 °C, and 45 s at 72 °C). Aliquots of PCR product were run on 1.5% agarose gels and then visualized by ethidium bromide staining. Lanes 1, 4, 7, 10, 13 and 16 are controls (medium alone); lanes 2, 5, 8, 11, 14 and 17 are 10 μg/ml hBD-2-stimulated samples, and lanes 3, 6, 9, 12, 15 and 18 are 0.001% DNCB-stimulated cells. Shown is one representative of five independent experiments. (B) Cells were stimulated with 10 μg/ml hBD-2 or 0.001% DNCB for 0.5–48 h, and the lysates were obtained by lysing cells in 40 μl lysis buffer (50 mM Tris–HCl (pH 8), 150 mM NaCl, 0.02% NaN_3, 0.1% SDS, 1% NP 40). The amounts of total protein were determined by BCA Protein Assay (Pierce Chemical, Rockford, IL) and equal amounts of total protein from stimulated or non-stimulated cells were analyzed by Western blot. The cell lysates were separated by SDS-PAGE on 15% polyacrylamide gel onto Immobilon-P membrane (Millipore, Bedford, MA). The membrane was stained with anti-human pro-IL-18 antibody (Research and Development Systems) at 1:1000-dilution, visualized with ECL Plus Kit (Amersham Biosciences, Buckinghamshire, UK). Lanes 1, 4, 7, 10, 13 and 16 are controls (medium alone); lanes 2, 5, 8, 11, 14 and 17 are 10 μg/ml hBD-2-stimulated samples, and lanes 3, 6, 9, 12, 15 and 18 are 0.001% DNCB-stimulated cells. The size of pro-IL-18 is 24 kDa. Shown is one representative of five independent experiments.

hBD-2 for 0.5–48 h (Fig. 2B). Similar observation has been reported after exposure of human keratinocytes to several inflammatory cytokines [6].

Up to now, the mechanism of IL-18 production by keratinocytes remains unclear. Although it is generally known that pro-IL-18 is cleaved by caspase-1 to generate a biologically active IL-18, a recent study on human keratinocytes has suggested that these cells constitutively produce pro-IL-18, but are unable to process it [8], assuming another pathway for IL-18 production. Indeed, a caspase-1-independent, Fas/Fas ligand-mediated IL-18 secretion from macrophages has been reported [10]. However, it is still unknown whether this pathway is involved in keratinocytes. Further study will be necessary to clarify the specific pathway involved in hBD-2-induced IL-18 secretion by keratinocytes.

In conclusion, the ability of hBD-2 to induce the secretion of IL-18 by keratinocytes suggests a new mechanism of the implication of human antibacterial peptides in innate and adaptive immunity, and their roles in the pathogenesis of certain skin diseases such as psoriasis and AD.

Acknowledgements

This work was supported in part by grants from the Ministry of Education, Culture, Sports, Science and Technology, Japan, and Atopy (Allergy) Research Center, Juntendo University, Tokyo, Japan. Dr. Sampanthanarak Pichai is supported by grants from Japan International Cooperation Agency (JICA).

References

[1] Weinberg A, Krisanaprakornkit S, Dale BA. Epithelial antimicrobial peptides: review and significance for oral applications. Crit Rev Oral Biol Med 1998;9:399–414.

[2] Niyonsaba F, Someya A, Hirata M, Ogawa H, Nagaoka I. Evaluation of the effects of peptide antibiotics human β-defensins-1/-2 and LL-37 on histamine release and prostaglandin D(2) production from mast cells. Eur J Immunol 2001;31:1066–75.

[3] Niyonsaba F, Ogawa H, Nagaoka I. Human beta-defensin-2 functions as a chemotactic agent for tumour necrosis factor-alpha-treated human neutrophils. Immunology 2004;111:273–81.

[4] Nakanishi K, Yoshimoto T, Tsutsui H, Okamura H. Interleukin-18 regulates both Th1 and Th2 responses. Annu Rev Immunol 2001;19:423–74.

[5] El-Mezzein RE, Matsumoto T, Nomiyama H, Miike T. Increased secretion of IL-18 in vitro by peripheral blood mononuclear cells of patients with bronchial asthma and atopic dermatitis. Clin Exp Immunol 2001;126:193–8.

[6] Naik SM, Cannon G, Burbach GJ, Singh SR, Swerlick RA, Wilcox JN, et al. Human keratinocytes constitutively express interleukin-18 and secrete biologically active interleukin-18 after treatment with pro-inflammatory mediators and dinitrochlorobenzene. J Invest Dermatol 1999;113:766–72.

[7] Nakano H, Tsutsui H, Terada M, Yasuda K, Matsui K, Yumikura-Futatsugi S, et al. Persistent secretion of IL-18 in the skin contributes to IgE response in mice. Int Immunol 2003;15:611–21.
[8] Mee JB, Alam Y, Groves RW. Human keratinocytes constitutively produce but do not process interleukin-18. Br J Dermatol 2000;143:330–6.
[9] Tone M, Thompson SA, Tone Y, Fairchild PJ, Waldmann HJ. Regulation of IL-18 (IFN-gamma-inducing factor) gene expression. J Immunol 1997;159:6156–63.
[10] Tsutsui H, Kayagaki N, Kuida K, Nakano H, Hayashi N, Takeda K, et al. Caspase-1-independent, Fas/Fas ligand-mediated IL-18 secretion from macrophages causes acute liver injury in mice. Immunity 1999;11:359–67.

Pichai Sampanthanarak[a,b]
François Niyonsaba[b,*]
Hiroko Ushio[b]
Isao Nagaoka[c]
Sigaku Ikeda[a]
Ko Okumura[d]
Hideoki Ogawa[a,b]

[a] *Department of Dermatology Juntendo University School of Medicine, 2-1-1 Hongo, Bunkyo-ku, Tokyo 113-8421, Japan*

[b] *Atopy (Allergy) Research Center Juntendo University School of Medicine 2-1-1 Hongo, Bunkyo-ku, Tokyo 113-8421, Japan*

[c] *Department of Host Defence and Biochemical Research, Juntendo University School of Medicine 2-1-1 Hongo, Bunkyo-ku, Tokyo 113-8421, Japan*

[d] *Department of Immunology, Juntendo University School of Medicine,2-1-1 Hongo Bunkyo-ku, Tokyo 113-8421, Japan*
*Corresponding author. Tel.: +81 3 5802 1591
fax: +81 3 3813 5512

21 October 2004

Mast Cells Acquire Monocyte-Specific Gene Expression and Monocyte-Like Morphology by Overproduction of PU.1[1]

Tomonobu Ito,*§ Chiharu Nishiyama,[2]* Makoto Nishiyama,¶ Hironori Matsuda,† Keiko Maeda,* Yushiro Akizawa,*‖ Ryoji Tsuboi,§ Ko Okumura,*† and Hideoki Ogawa*‡

PU.1 is a myeloid- and lymphoid-specific transcription factor that belongs to the Ets family. Recently, we found that overproduction of PU.1 in mouse bone marrow-derived hemopoietic progenitor cells induced monocyte-specific gene expression and caused their monocyte-like morphological change. In the present study, PU.1 was overproduced by using retrovirus expression system in differentiated bone marrow-derived mast cells. By overexpression of PU.1, cell surface expression of MHC class II, CD11b, CD11c, and F4/80 was induced, accompanied by reduced expression of c-*kit*, a mast cell-specific marker. Morphology of PU.1-transfected cells was altered toward monocyte-like one. PU.1-overproducing cells acquired T cell stimulatory ability and showed an increase in response to LPS stimulation, while response through FcεRI was markedly reduced by overproduction of PU.1. These results suggest that the differentiated mast cells still have potential to display monocytic features. When PU.1 was overproduced in a different type of mast cell, peritoneal mast cells, similar monocyte-like morphological change, and the expression of CD11b and F4/80 were induced. However, surface level of CD11c and MHC class II was not affected. These results indicate that the potential capacity to exhibit monocytic features is different between both the mast cells. *The Journal of Immunology*, 2005, 174: 376–383.

PU.1 is an Ets family transcription factor and involved in lymphoid and myeloid cell development and specific gene regulation. PU.1 is expressed in lymphoid cells, macrophages, dendritic cells (DC),[3] neutrophils, and mast cells in a cell type-specific manner (1). The necessity of PU.1 for generation of these lineages was shown by PU.1 knockout mouse that abolishes macrophage and B cell production and delays neutrophil and T cell production (2–4). The requirement of PU.1 for the development of DC and mast cells was also recently revealed by the analyses using PU.1 knockout mouse (5–7). It was also reported that expression level of PU.1 determines cell fate between B cells/macrophages (8) and neutrophils/macrophages (9). In addition, recent analyses demonstrated that overexpression of PU.1 in $CD34^+$ human myeloid progenitors triggers development of Langerhans cells (LC) (10, 11).

Recently, we found that overproduction of PU.1 in mouse bone marrow-derived hemopoietic progenitor cells developing toward mast cells induced the expression of several monocyte-specific genes and caused morphological change (12). In this study, we conducted overexpression of PU.1 by retrovirus transfection system in differentiated mast cells, mouse bone marrow-derived mast cells (BMMC), and peritoneal mast cells (PMC), and examined its effect on the expression of monocyte- and mast cell-specific markers and the cell morphology. BMMC and PMC showed several monocytic characteristics by overproduction of PU.1, suggesting that PU.1 functions to promote monocyte-specific gene expression even in developed mast cells, and that developed mast cells still possess the potential capacity to exhibit several monocytic features.

Materials and Methods

Cells

A retrovirus packaging cell, Plat-E (13), was maintained in DMEM (Sigma-Aldrich) supplemented with 10% heat-inactivated FBS (Sigma-Aldrich), 100 U/ml penicillin, 100 μg/ml streptomycin, 1 μg/ml puromycin (Sigma-Aldrich), and 10 μg/ml blasticidin (Funakoshi). To generate BMMC, bone marrow cells prepared from BALB/c (Japan SLC, Hamamatsu, Japan) were grown in RPMI 1640 (Sigma-Aldrich) supplemented with 10% heat-inactivated FBS, 100 μM 2-ME, 10 μM MEM nonessential amino acids solution (Sigma-Aldrich), 100 U/ml penicillin, 100 μg/ml streptomycin, and 10% pokeweed mitogen-stimulated spleen-condition medium (14). After 4-wk culture, >95% of cells were identifiable as mast cells by toluidine blue staining and as c-kit^+/FcεRI$^+$ by flow cytometric analysis. Mouse PMC was prepared from whole peritoneal cells by density-gradient centrifugation techniques using metrizamide (Sigma-Aldrich) with >98% purity (15), and was maintained in RPMI 1640 supplemented with 10% FBS, 10% pokeweed mitogen-stimulated spleen-condition medium, 20 ng/ml mouse recombinant stem cell factor (PeproTech), and antibiotics (penicillin and streptomycin). Bone marrow-derived DC (BMDC) was prepared according to previously reported method (16, 17), with some modifications. In brief, bone marrow cells prepared from BALB/c were grown in RPMI 1640 supplemented with 10% FBS, 100 μM 2-ME, 10 μM MEM nonessential amino acids solution, antibiotics, 10 ng/ml mouse rGM-CSF (PeproTech), and 10 ng/ml mouse rIL-4 (PeproTech). Peritoneal macrophages were obtained from BALB/c, as described previously (18). Briefly, peritoneal exudate cells were harvested from mice, which received i.p. 2 ml of 4% thioglycolate (Sigma-Aldrich) 4 days before, by peritoneal lavage with ice-cold PBS. After 1-h culture on a plastic dish, nonadherent cells were collected and used as peritoneal macrophages.

Plasmid construction

Plasmids, pMX-puro-PU.1 (12), and pMX-puro (19) were used to generate retrovirus vector to overproduce PU.1 tagged with 2× Flag at N terminus as per our previous reports (12, 20). The 2× Flag-tagged PU.1 cDNA sequence was isolated from pCR-2F-PU.1 (21) and subcloned into

*Atopy (Allergy) Research Center, †Department of Immunology, and ‡Department of Dermatology, Juntendo University School of Medicine, Tokyo, Japan; §Department of Dermatology, Tokyo Medical University, Tokyo, Japan; ¶Biotechnology Research Center, University of Tokyo, Tokyo, Japan; and ‖Advanced Research Laboratory, Hanno Research Center, Taiho Pharmaceutical, Saitama, Japan

Received for publication May 4, 2004. Accepted for publication November 1, 2004.

The costs of publication of this article were defrayed in part by the payment of page charges. This article must therefore be hereby marked *advertisement* in accordance with 18 U.S.C. Section 1734 solely to indicate this fact.

[1] This work was supported in part by a Grant-in-Aid for Young Scientists from the Ministry of Education, Culture, Sports, Science, and Technology of Japan (to C.N.).

[2] Address correspondence and reprint requests to Dr. Chiharu Nishiyama, Atopy (Allergy) Research Center, Juntendo University School of Medicine, 2-1-1 Hongo, Bunkyo-ku, Tokyo, 113-8421, Japan. E-mail address: chinishi@med.juntendo.ac.jp

[3] Abbreviations used in this paper: DC, dendritic cell; BMDC, bone marrow-derived DC; BMMC, bone marrow-derived mast cell; LC, Langerhans cell; PGN, peptidoglycan; PMC, peritoneal mast cell.

0022-1767/05/$02.00

pMX-IG (22) using restriction endonucleases and a DNA ligation kit, version 1 (Takara BIO), to generate pMX-IG-PU.1.

Transfection

Infection of BMMC and PMC was performed, according to a previously reported method (12, 20). In brief, pMX-puro (mock vector) and pMX-puro-PU.1 (for the expression of wild-type PU.1) were transiently introduced into Plat-E with Fugene6 (Roche Diagnostics). BMMC after 4-wk culture and freshly prepared PMC were incubated with harvested culture medium of transfected Plat-E containing infectious viruses for 2 days in the presence of 10 μg/ml polybrene (Sigma-Aldrich). Infected cells were selected by culture in the presence of 1.2 μg/ml puromycin for 10–20 days. When pMX-IG and pMX-IG-PU.1 were used for transfection, transfectants that were obtained by the same method as that of pMX-puro-series described above were selected as GFP-positive cells.

Western blotting analysis

To detect endogenous PU.1, BMMC was stimulated by 1 μg/ml LPS or 100 mg/ml PMA (Sigma-Aldrich) for 0–48 h. Whole cells were subjected to Western blotting analysis. Rabbit polyclonal Ab against PU.1 (Santa Cruz Biotechnology) or mouse mAb against Flag-tag (Sigma-Aldrich) was used as the primary Ab. Alexa Fluor 680 goat anti-rabbit IgG or Alexa Fluor 680 goat anti-mouse IgG (Molecular Probes) was used as the secondary Ab. Infrared fluorescence on membranes was detected by Odyssey infrared imaging system (model ODY-9201-SC; LI-COR).

Flow cytometric analysis

The FITC- or PE-conjugated anti-mouse Abs against I-A^d, CD11b, CD11c, F4/80, and c-*kit*, all of which were purchased from BD Pharmingen, were used to stain each cell surface molecule after blocking Fc receptors with 2.4G2 (BD Pharmingen). Mouse IgE Ab (BD Pharmingen) conjugated with FITC was used to stain mouse FcεRI. To stain TLR2 and 4, anti-mouse TLR2 and 4 rat IgG mAbs purchased from HyCult Biotechnology were used as the first Ab, respectively, and FITC-conjugated rabbit $F(ab')_2$ anti-rat IgG Ab (Valeant Pharmaceuticals) was used as the second Ab. In the case of pMX-IG-series transfectants expressing GFP, cells were stained with PE-conjugated anti-mouse c-*kit* and allophycocyanin-conjugated anti-mouse CD11b, CD11c, or combination of biotin-labeled anti-mouse I-A^d and streptavidin-allophycocyanin (BD Pharmingen). For sorting of c-*kit*-positive or c-*kit*/FcεRI-double-positive cells, BD FACSAria Cell Sorter (BD Biosciences, San Jose, CA) was used. Cells stained with each Ab, as described previously (23, 24), were analyzed by FACSCalibur flow cytometer (BD Biosciences).

Morphological analysis

Electron microscopy and May-Grünwald-Giemsa's staining were performed, as described previously (12).

LPS, peptidoglycan (PGN), and Ag/IgE stimulation

Culture medium of cells stimulated with LPS (from *Escherichia coli*; Sigma-Aldrich), PGN (from *Staphylococcus aureus*; Sigma-Aldrich), or Ag/IgE was harvested after 6-h incubation. Stimulation with Ag/IgE was performed according to a previously published method (25). Concentrations of IL-6 in the culture supernatant were determined by an ELISA kit, according to the manufacturer's instruction (Genzyme Techne, Minneapolis, MN). β-Hexosaminidase-releasing assay was performed with previously reported method (25) to investigate degranulation activity.

Ag presentation assay

Cells irradiated at a dose of 30 Gy were plated into 96-well round-bottom plates at 5-fold serial dilutions, each well of which contained splenic $CD4^+$ T cells from C57BL/6 mice at 3×10^5, and incubated for 2 days. [^{3}H]Thymidine was then added (0.37 Mbq/well), and incubation was continued for an additional 15 h.

Results

*Overproduction of PU.1 in BMMC induced the expression of MHC class II, CD11b, CD11c, and F4/80, and suppressed the expression of c-*kit

To examine the effect of overproduced PU.1 in mast cells, BMMC were transfected with retrovirus vector that directed the production of wild-type PU.1 or empty vector (Fig. 1*A*). In Western blotting analysis using anti-PU.1 Ab (Fig. 1*B*), apparent production of wild-type PU.1 was observed, while endogenous PU.1 was not detected under the conditions used (see Fig. 1*B*, control (without transfection) and mock), indicating that the cells transfected with pMX-puro-PU.1 expressed much larger amount of PU.1 than that of endogenous PU.1. BMMC (*top panel* of Fig. 1*C*) and mock transfectants (*second panel* of Fig. 1*C*) expressed mast cell-specific markers (FcεRI and c-*kit*), but not monocyte-specific molecules (MHC class II, CD11b, CD11c, and F4/80; *bottom panel* of Fig. 1*C*) on cell surface. In contrast, overproduction of PU.1 in BMMC induced the expression of MHC class II, CD11b, CD11c, and F4/80, while the expression of c-*kit* was slightly suppressed (*third panel* of Fig. 1*C*). Significant difference was not observed in the expression level of FcεRI. These results indicated that overproduction of PU.1 in BMMC induced the expression of monocyte-specific molecules and suppressed c-*kit* expression.

Morphology of transfectants

To investigate the effect of PU.1 overproduction on the morphology of the cells, May-Grünwald-Giemsa staining of cytospun (Fig. 2*A*) and electron microscopy (Fig. 2*B*) were performed. The mock transfectants contained a large amount of granules as well as control BMMC. In contrast, PU.1-overproducing cells contained lesser amount of granules, but showed macrophage- and DC-like morphology characterized by vacuoles in the cytoplasm, larger veils, and lamellipodia extending from cell bodies. These observations showed that overproduction of PU.1 caused monocyte-like morphological change on BMMC.

Response to LPS and PGN stimulation

TLR4 signaling activated by LPS induces DC and macrophages to produce proinflammatory cytokines, including IL-6 (26). Although mast cells also produce IL-6 in response to LPS, the production level is quite lower than that of monocytes (27). We therefore analyzed the IL-6 production level of PU.1-overproducing cells by LPS stimulation (Fig. 3*A*). The amount of IL-6 produced by LPS stimulation was markedly increased in cells overproducing wild-type PU.1 as well as BMDC. In contrast, mock transfectants produced IL-6 at the level similar to that of BMMC.

To confirm the specificity of TLR signaling, we next analyzed the response to PGN, which activates cells via TLR2, by measuring IL-6 released from each transfectant (Fig. 3*B*). Overproduction of PU.1 resulted in markedly increased production of IL-6 in response to PGN stimulation.

Recently, it has been reported that the essential elements in the promoters of TLR2 and 4 genes were recognized by PU.1 (28, 29), suggesting the possibility that overproduction of PU.1 might enhance IL-6 production through increased expression of TLR2 and 4. We therefore analyzed cell surface expression of TLR2 and 4 in PU.1-overproducing cells (Fig. 3*C*). Although bone marrow-derived DC expressed an apparent amount of TLR2 and 4, PU.1-overproducing cells expressed TLR2 and 4 only slightly, which was similar to the case in BMMC.

These results suggest that PU.1 enhances IL-6 production by activating downstream process of TLR-LPS/PGN interaction in TLR signaling, but not by increasing the expression of TLRs.

Response to Ag/IgE stimulation

Mast cells also produce IL-6 in response to Ag/IgE stimulation through FcεRI. Although a certain kind of monocyte expresses FcεRI, the response of monocytes through FcεRI is markedly reduced in comparison with that of mast cells (30). To examine the effect of PU.1 on response to Ag/IgE stimulation, we analyzed the level of IL-6 production of the cells stimulated by Ag/IgE (Fig. 4*A*). The amount of IL-6 produced from PU.1-overproducing cells was markedly reduced when compared with the case of mock

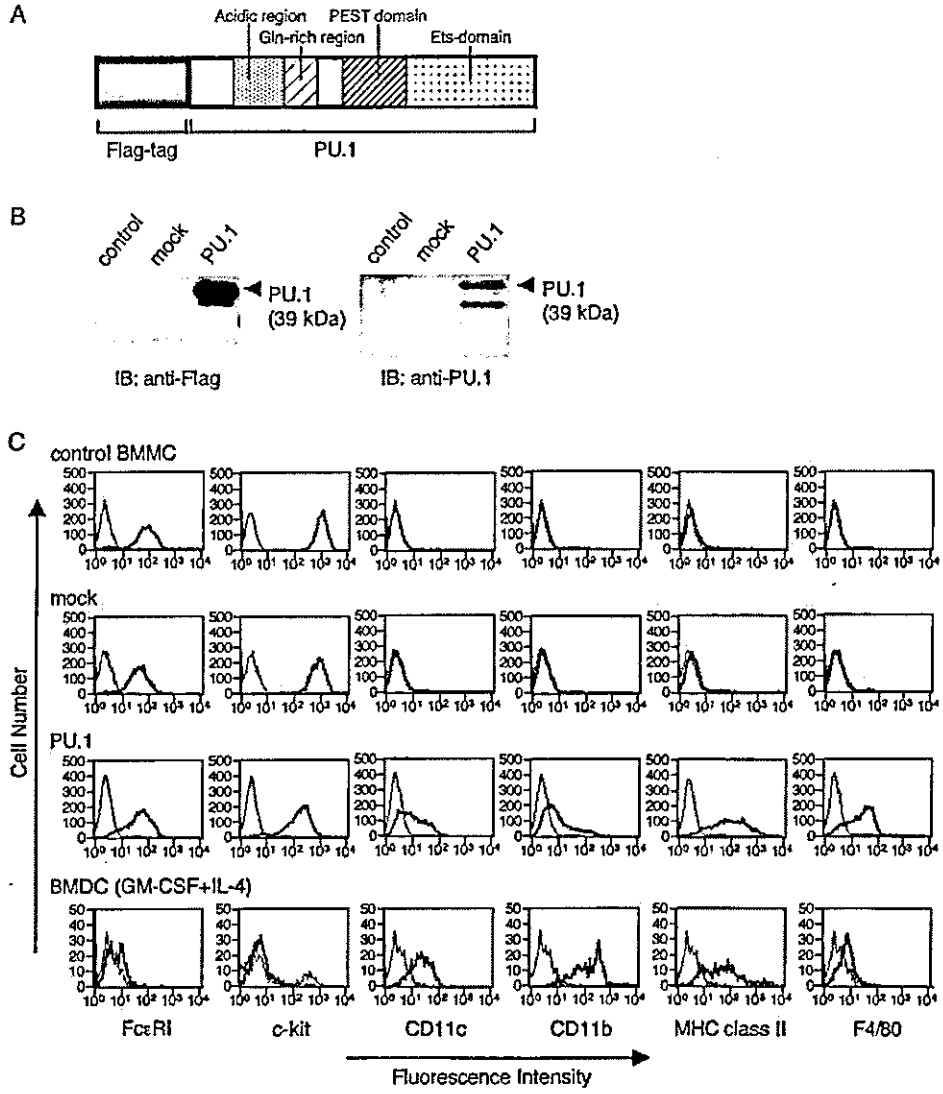

FIGURE 1. Overexpression of PU.1 in BMMC induces monocyte-specific gene expression. *A*, Schematic structure of PU.1. PU.1 is composed of the acidic region (33–73), the Gln-rich region (74–99), the Pro, Glu, Ser, and Thr-rich (PEST) region (117–166), and the Ets domain (167–271). The amino acid residue numbers are that of rat PU.1 numbering (21). PU.1 that is overproduced by retrovirus vector is tagged with 2× Flag at its N terminus. *B*, Western blotting analysis of BMMC and transfectants. A total of 5×10^5 cells was applied onto each lane. Control, normal BMMC after 6-wk culture; mock, BMMC transfected with mock vector (pMX-puro); PU.1, BMMC transfected with retrovirus vector encoding PU.1 cDNA (pMX-puro-PU.1). Transfectants were selected as puromycin-resistant cells by 10- to 20-day culture in the presence of puromycin (1.2 μg/ml). *C*, Cell surface expression of mast cell- and monocyte-specific molecules. Thick-line histogram represents cells with each Ab. Thin-line histogram indicates control with 2.4G2 alone. Control (*top panel*), normal BMMC without infection; mock (*second panel*), BMMC transfected with pMX-puro; PU.1 (*third panel*), BMMC transfected with pMX-puro-PU.1; BMDC (*bottom panel*), mouse BMDC. A representative result of five independent experiments is shown.

transfectants and control BMMC. This result indicated that overproduction of PU.1 reduced IL-6 production by interfering the signal from FcεRI.

Degranulation by cross-linking of FcεRI is one of the major characteristics of mast cells. Therefore, degranulation of the cells overproducing PU.1 was analyzed (Fig. 4*B*). Control BMMC and mock transfectants were degranulated by stimulation with Ag/IgE to the same degree. In contrast, degranulation of the cells overproducing PU.1 was markedly decreased as well as BMDC.

From these results, it was concluded that overproduction of PU.1 reduced response to the stimulation through FcεRI in mast cells.

T cell stimulation activity

Overproduction of PU.1 induced marked expression of MHC class II, which is a hallmark of APCs, on mast cells, as shown in Fig. 1*C*. To examine whether induced MHC class II possesses function, allostimulatory activity of transfectants cocultured with allogenic C57BL/6 $CD4^+$ T cells was measured. Thymidine incorporation of T cells was significantly increased when PU.1-overproducing cells were cocultured (Fig. 5).

Effect of overproduction of PU.1 on PMC

PMC is connective tissue-type mast cell, which is more maturated than mucosal-type mast cell, BMMC. To examine the effect of PU.1 on connective tissue-type mast cells, PU.1 was overexpressed in freshly isolated PMC by the retrovirus vectors. The expression level of PU.1 in transfectants was increased, as was the case in BMMC (data not shown). May-Grünwald-Giemsa staining indicated that overproduction of PU.1 caused morphological change of the cells: decrease in granules accompanied by formation of vacuoles, larger veils, and lamellipodia (Fig. 6*A*). Expression profile of the cell surface markers on PU.1-overproducing PMC (Fig. 6*B*) was somewhat different from the case of BMMC. Similar to the case in BMMC, CD11b and F4/80 were expressed and c-*kit* expression was suppressed on PU.1-overproducing PMC. However, expression of CD11c and MHC class II was not induced in the transfectant. Thus, increased expression of PU.1 induced several monocyte-like changes even in PMC, but the effect of PU.1 was negligible on some target molecules such as CD11b and MHC class II in PMC.

Transfection of sorted mast cells using internal ribosome entry site-GFP system to eliminate the contamination of monocyte lineages

Ten- to 20-day culture was required to select transfectants by puromycin, when plasmids pMX-puro-series were used for retrovirus transfection, as described above. Although the purity of mast cells is high (>95% for BMMC and >98% for PMC, as described in *Materials and Methods*), the possibility that monocytes and/or

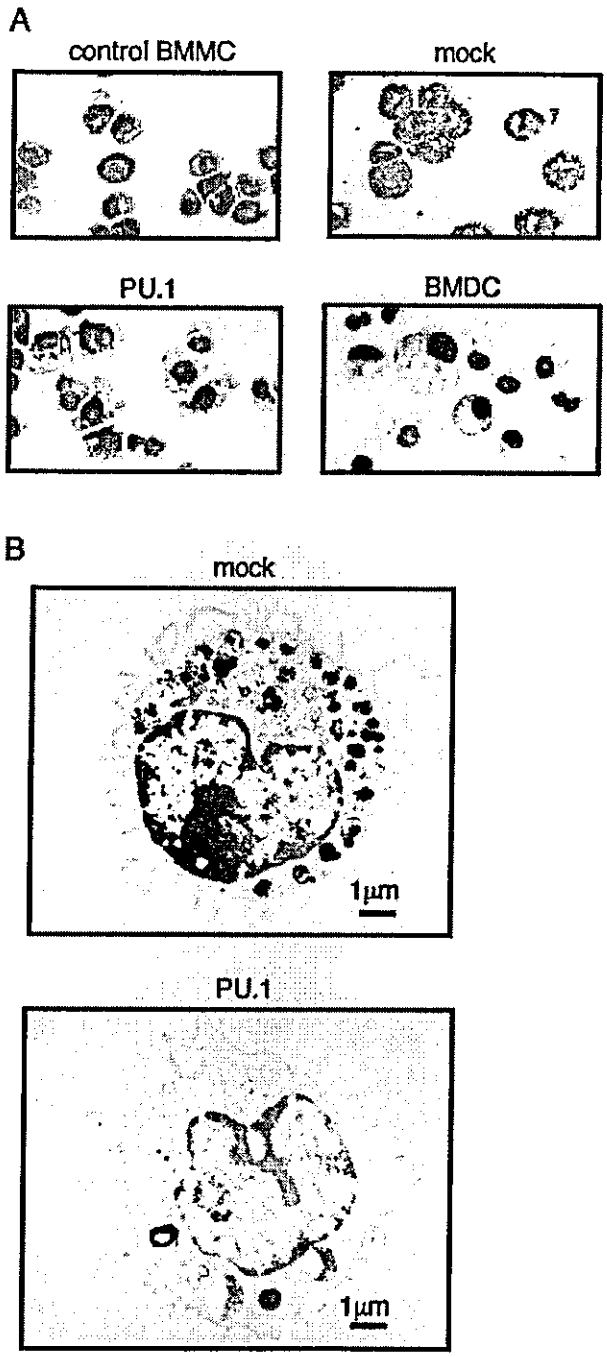

FIGURE 2. Morphology of control BMMC, each transfectant, and BMDC. *A*, May-Grünwald-Giemsa staining. ×1000. *B*, Electron micrographs; ×6000.

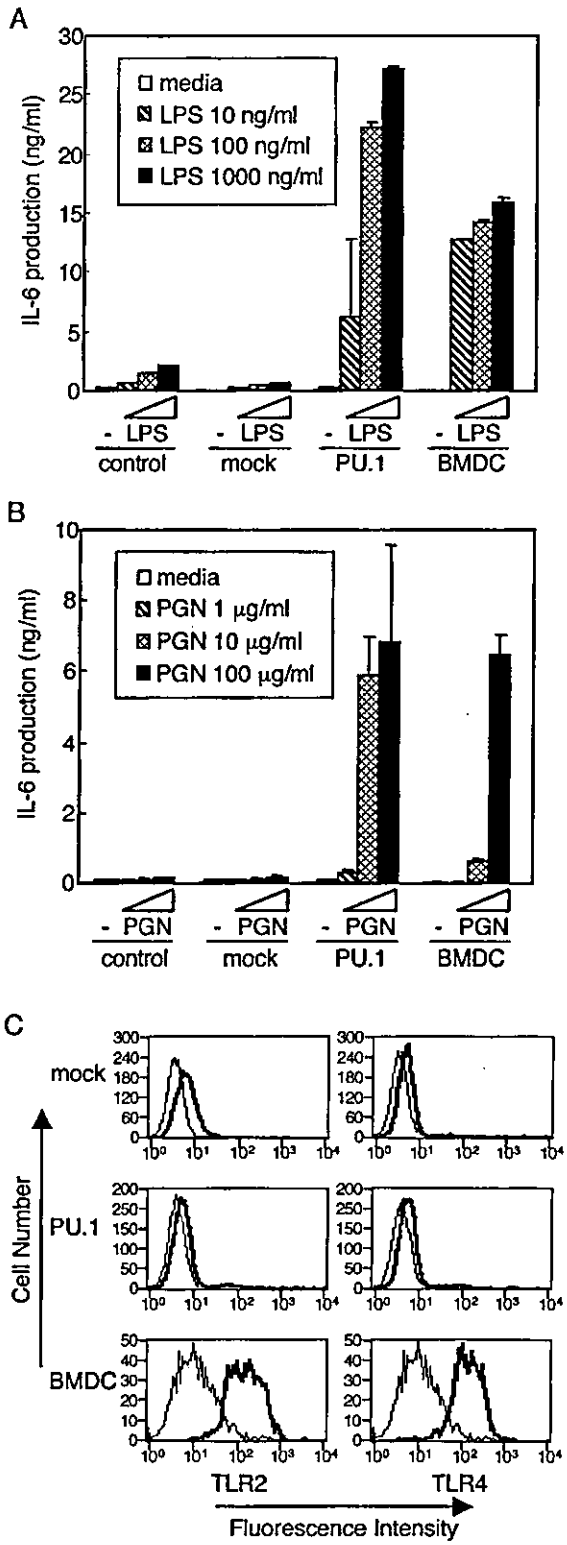

FIGURE 3. IL-6 production in response to the stimulation through TLR2 and 4. IL-6 production level in response to LPS stimulation (*A*) and PGN stimulation (*B*) was enhanced by overproduction of PU.1, whereas cell surface expression level of TLR2 and 4 was not affected by overproduction of PU.1 (*C*). *A* and *B*, IL-6 concentration in culture medium after 6 h of stimulation was measured by ELISA. A representative result performed with triplicate was shown as mean ± SD. Similar results were observed in other three independent experiments. *C*, Histogram of thick line represents cells stained with anti-TLR2 or 4 as first Ab and FITC-conjugated anti-rat IgG Ab as second Ab. Thin-line histogram indicates control cells incubated with second Ab alone. Similar profile was observed in another independent experiment.

monocyte progenitors contaminated mast cell suspensions could not be excluded completely. This issue raised a possibility that contaminating monocytes and/or monocyte progenitors that were transfected with retrovirus directing to produce PU.1 proliferated more vigorously than transfected mast cells in the culture period. Therefore, to eliminate this possibility, we used purified BMMC that was collected as c-*kit*$^+$/FcεRI$^+$ cells by sorting for transfection. After 14-day culture for selection of transfectants, >98% of mock transfectants were c-*kit*$^+$/FcεRI$^+$, while c-*kit*$^+$/FcεRI$^+$ population of ~94% was obtained from PU.1 transfectant (Fig. 7*A*). PU.1-overproducing cells expressed CD11c, CD11b, and MHC class II, which were not expressed on mock transfectants. These

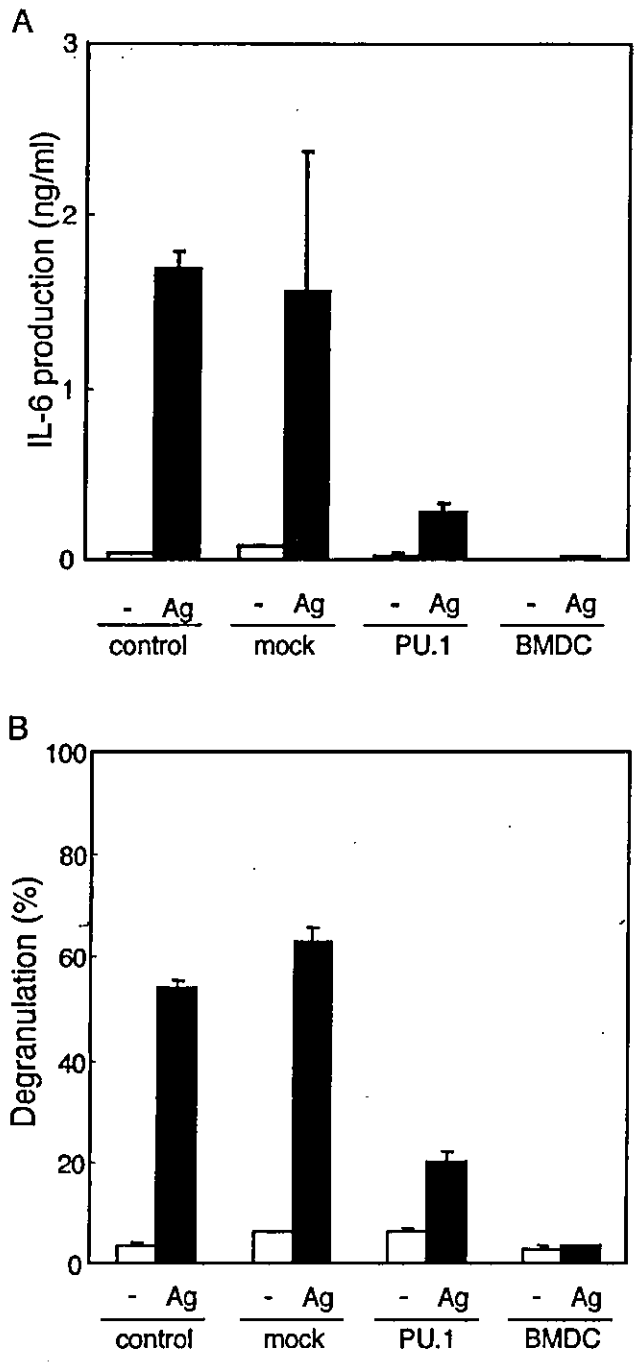

FIGURE 4. Response to Ag/IgE stimulation through FcεRI. *A*, IL-6 production of control or transfected BMMC. IL-6 concentration in culture medium after 6 h of stimulation by Ag/IgE was measured by ELISA. □, Cells were incubated with IgE Ab, but not following addition of Ag (DNP-BSA); ■, cells were cross-linked with Ag after incubation with IgE Ab. *B*, β-Hexosaminidase released from control or transfected BMMC. β-Hexosaminidase activity in supernatant was measured after 1-h incubation from stimulation by Ag/IgE. □, Cells were incubated with IgE Ab, but not following addition of Ag (DNP-BSA); ■, cells were cross-linked with Ag after incubation with IgE Ab. A representative result performed with triplicate was shown as mean ± SD in *A* and *B*. Similar results were observed in three other independent experiments.

results were consistent with the results of BMMC without sorting (Fig. 1*C*). In addition, CD11c-, CD11b-, and MHC class II-positive cells also expressed mast cell markers, c-*kit* and FcεRI. This result suggested that the cells expressing CD11c, CD11b, and MHC class II originated from mast cells.

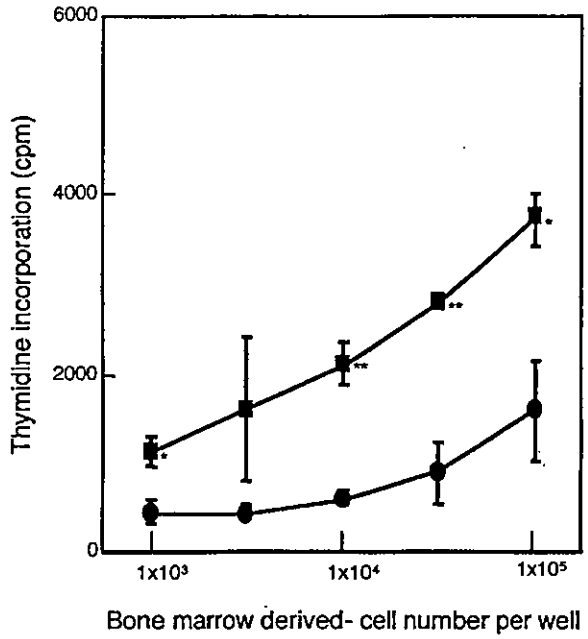

FIGURE 5. Effect of PU.1 on allostimulatory activity. Transfectants (H-2d) were irradiated and incubated with allogeneic $CD4^+$ T cells (H-2b) at the indicated concentrations. Proliferative responses of T cells were evaluated by the [^{3}H]thymidine incorporation of $CD4^+$ T cells. The results are expressed as mean ± SD of triplicate samples. *, $p < 0.005$; **, $p < 0.001$, as determined by a paired *t* test.

To eliminate the possibility that a few contaminating monocytes and/or its progenitors grew as a major population through 20 days of culture, we constructed plasmids, pMX-IG and pMX-IG-PU.1. By infection with retrovirus, transfectants were detected as GFP^+ cells within 2 days after transfection (Fig. 7*B*). GFP^+ population of BMMC infected with the retrovirus generated from pMX-IG-PU.1 showed reduced expression of c-*kit*, while GFP^- population and GFP^+ mock expressed c-*kit* at the level same as that of GFP^- mock. PU.1-overproducing cells detected as GFP^+ expressed CD11c and MHC class II, while most of the GFP^+ population of mock transfectants did not express these molecules. These observations excluded the possibility that contaminating monocytes were the source of cells expressing monocyte-specific molecules. From these results, we concluded that overproduction of PU.1 in BMMC suppressed c-*kit* expression and induced the expression of CD11c and MHC class II.

Up-regulation of endogenous PU.1 in mast cells by LPS or PMA stimulation

Because PU.1 autoregulates its own promoter (31), the stimulation signal to activate PU.1 protein would further accelerate overexpression of PU.1. Actually, the signal to activate PU.1 protein by LPS (32) and PMA (33) induces the up-regulation of PU.1 in monocytes. Therefore, we hypothesized that mast cells and/or its progenitors might be converted to monocyte-like cells in vivo under a certain condition when either activation or up-regulation of PU.1 is induced. To evaluate the effect of LPS and PMA on PU.1 expression level in mast cells, endogenous PU.1 proteins were analyzed after stimulation of mast cells with LPS or PMA by Western blotting. Intensity of the band migrating at ~39 kDa was markedly increased from 4 h after LPS or PMA stimulation and decreased to background level by 24-h incubation (Fig. 8). An additional band migrating slower than the major band of ~43 kDa also appeared from 4 to 8 h after LPS or PMA stimulation. Considering that PU.1 is shown to be present in several forms with

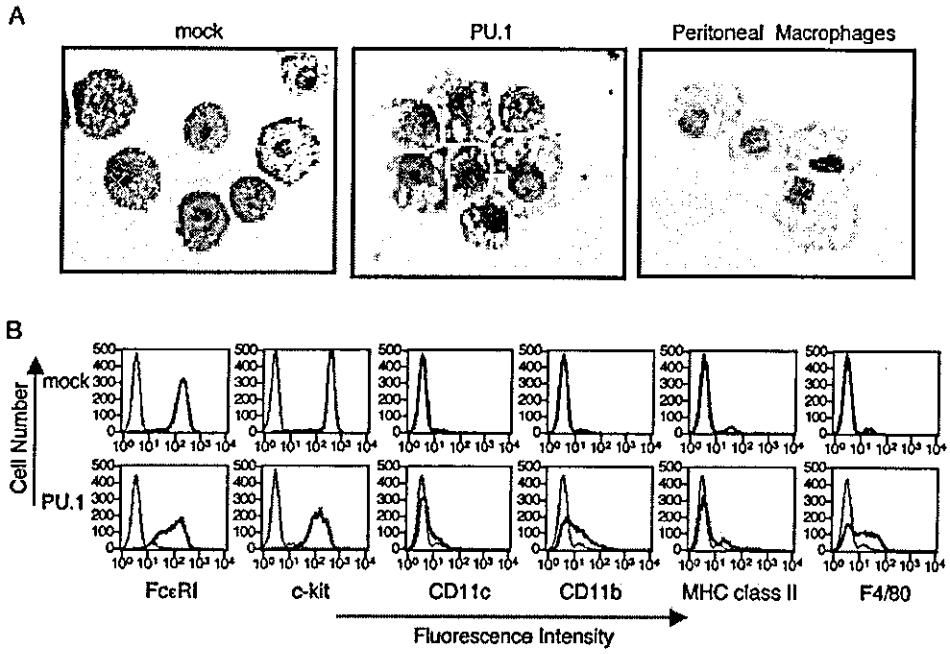

FIGURE 6. Overproduction of PU.1 in PMC. *A*, May-Grünwald-Giemsa staining of transfected PMC and peritoneal macrophages. ×1000. *B*, Cell surface expression of mast cell- or monocyte-specific molecules. Thick-line histogram represents cells with each Ab. Thin-line histogram indicates control with 2.4G2 alone.

various apparent molecular mass (from 38.5 to 46.5 kDa) (1), it is likely that proteins that were recognized by anti-PU.1 Ab are PU.1. Therefore, these results indicate that endogenous PU.1 in mast cells is potentially up-regulated in a certain condition, such as stimulation with LPS or PMA.

Discussion

PU.1 is a transcription factor involved in the lymphoid- and myeloid-specific gene regulation and the development of these cell lineages. Expression level of PU.1 determines cell fate between B cells/macrophages (8) and neutrophils/macrophages (9). In addition, overexpression of PU.1 in $CD34^+$ human myeloid progenitors promotes LC development (10, 11). In recent analysis, we found that monocyte-specific gene expression and monocyte-like morphological change were induced by overproduction of PU.1 in mouse bone marrow-derived mast cell progenitors (12, 20, 21). In this study, overproduction of PU.1 caused several monocyte-like characteristics on both BMMC and PMC, suggesting that developed mast cells still have the capacity to exhibit monocyte-like features.

Although the overproduction of PU.1 decreased the function and morphology of mast cells, PU.1 overproduction did not decrease the expression of FcεRI, a typical marker for mast cells. In most cases, PU.1 inhibits GATA-1 to function and vice versa, possibly by forming an inactive PU.1/GATA-1 complex (34), and therefore, only either PU.1 or GATA-1 is expressed in a cell. For example, in monocyte/granulocyte lineage development from hemapoietic stem cells, stimulation signals such as GM-CSF up-regulates PU.1 expression, which subsequently inhibits the function of GATA-1 in these cells (34–36). However, mast cells produce both PU.1 and GATA-1, and both transcription factors *trans* activate the promoter of FcεRI α-chain (37). GATA-1 also positively regulates the transcription of another FcεRI-specific component, FcεRI β-chain (38). In our present study, we observed that BMMC transfectants overproducing PU.1 still expressed GATA-1 at similar level as that of mock transfectants (data not shown). Therefore, we assume that GATA-1 present in the cell might assure FcεRI expression even in BMMC overproducing PU.1. The mechanism allowing the copresence of both GATA-1 and PU.1 in mast cells is unclear at present. Considering that cooperative function between GATA-1 and PU.1 is involved in mast cell-specific gene regulation (7, 37, 39), we speculate that this synergistic effect may be essential for mast cell development. In any case, further detailed analysis will be required to clarify these points.

Overproduction of PU.1 induced apparent expression of CD11b and F4/80, and suppressed c-*kit* expression in PMC. However, the PU.1 overproduction did not induce expression of CD11c and MHC class II in PMC, which was in contrast to the case of BMMC overproducing PU.1. These results indicated that PMC possessed lower capacity to express monocyte-specific gene than that of BMMC. We assume that this discrepancy may reflect the difference in the expression profile of other transcription factors between these cells. A transcription factor, C/EBPα, might be one of the candidates, because C/EBPα is reported to inhibit development of myeloid progenitor cells to DC, which is induced by PU.1, and direct them to macrophage and granulocyte lineages (11).

Overexpression of PU.1 in BMMC induced hyperproduction of IL-6 in response to stimulation signal through TLR2 and 4. It is suggested that PU.1 is involved in the transcriptional regulation of TLR2 and 4 (28, 29). However, expression level of TLR2 and 4 in BMMC was not affected by overproduction of PU.1 (Fig. 3). In addition, production of IL-6 in response to Ag/IgE stimulation was reduced (Fig. 4*A*). These results suggest that PU.1 regulates IL-6 expression in a complex manner. Considering that PU.1 is activated by stimulation with LPS (32), PU.1 might function in the downstream process in TLR signaling.

PU.1 autoregulates its own promoter (31). Therefore, the stimulation signal to activate PU.1 protein would further accelerate up-regulation of PU.1. Therefore, we hypothesize that mast cells and/or its progenitors might be converted to monocyte-like cells in vivo under a certain condition when either activation or overproduction of PU.1 is induced. We have shown that LPS and PMA stimulation induced PU.1 production in mast cells, which suggests that mast cells might be potential sources for macrophages and/or DC under certain conditions in vivo. This is the first observation in mast cells showing up-regulation of PU.1 by stimulation of LPS and PMA. However, the production of PU.1 induced by LPS or PMA stimulation was transient and markedly lower in level than that of PU.1 produced by retrovirus system. We assume that this is the reason for failure of the stimulations in converting mast cells to

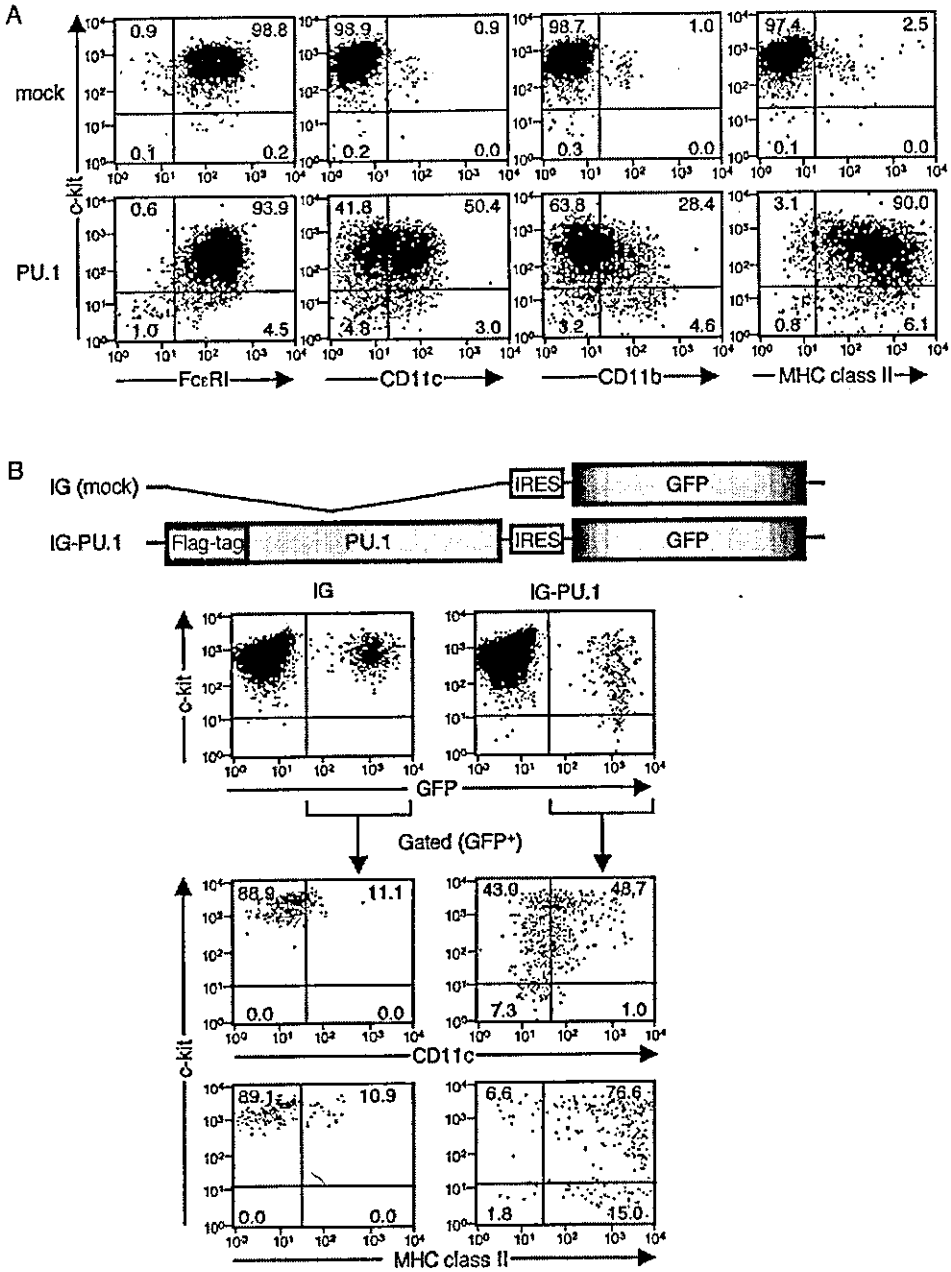

FIGURE 7. Effect of PU.1 overproduction on the expression of monocyte-specific markers for highly purified mast cells. *A*, Overproduction of PU.1 in BMMC highly purified by cell-sorting system with c-*kit*$^+$/FcεRI$^+$ as markers. c-*kit*$^+$/FcεRI$^+$ cells were transfected with pMX-puro or pMX-puro-PU.1. Transfectants resistant to puromycin were selected through 10-day culture in the presence of puromycin, and were double stained with PE-labeled anti-c-*kit* mAb and either FITC-labeled anti-FcεRIα, anti-CD11c, anti-CD11b, or anti-I-A^d mAb. *B*, PU.1-internal ribosome entry site (IRES)-GFP system. c-*kit*$^+$ cells collected by cell-sorting system were transfected with pMX-IG or pMX-IG-PU.1. Transfectants were monitored as GFP$^+$ cells 2 days after infection. Cells were double stained with PE-labeled anti-c-*kit* mAb and either allophycocyanin-labeled anti-CD11c mAb or biotinylated anti-I-A^d mAb, followed by allophycocyanin-labeled streptavidin. The GFP$^+$ populations in the *top panels* were electronically gated, and their dot plots of double stain were shown in the *middle panels* (PE-c-*kit* plus allophycocyanin-CD11c) and in the *bottom panels* (PE-c-*kit* plus biotin-I-A^d/allophycocyanin-avidin).

monocytes. To prove this possibility, further analysis will be required to optimize conditions of PU.1 induction in mast cells, which are suitable for obtaining monocyte-specific gene expression.

Recently, the presence in vivo of FcεRI-positive monocytes, DC, and LC, all of which possess the Ag presentation ability, was shown (40, 41). Considering that the marked up-regulation of FcεRI expression is observed specifically on LC and DC in lesional skin of atopic dermatitis (40, 41), we assume that above-mentioned signal to activate PU.1 might be a possible cause of the appearance of FcεRI-positive monocytes, which are developed from mast cells or its progenitors in vivo. Therefore, characterization of the mechanisms for the regulation of FcεRI expression on monocyte might give important information for prevention of atopic dermatitis.

GM-CSF (16) and M-CSF (42) induce development of hemopoietic progenitor cells toward DC and macrophage. In the process of monocyte development, the signal through these factors is transduced to Fes and subsequently to PU.1 (43) to induce the expression of the receptors for GM-CSF (44) and M-CSF (45). Actually, retrovirus-mediated expression of PU.1 in macrophage prepared from GM-CSF-null mice rescued the defect in differentiation (46). Thus, it is likely that PU.1-mediated gene expression is a key event in monocyte development. However, the mechanism for both activation of PU.1 and up-regulation of PU.1 expression is mostly unknown. Therefore, further detailed analyses on upstream and downstream signaling of PU.1 are required for revealing the mechanism for monocyte lineage development.

Acknowledgments

We thank Dr. M. Yoshida for electron microscopy, Dr. K. Yokomizo for May-Grünwald-Giemsa staining, Dr. T. Sakanishi for operating the cell-sorting system, and Drs. T. Kitamura and H. Nakano for providing Plat-E and pCR-2F, respectively. We are grateful to members of Atopy (Allergy) Research Center, Department of Immunology, and Department of Dermatology for helpful discussions, especially Drs. H. Yagita, A. Nakao (University of Yamanashi, Yamanashi, Japan), H. Ushio, H. Akiba, and T. Yamazaki. We thank Drs. N. Nakano, H. Kawada, A. Takagi, and A. Okamoto, and K.

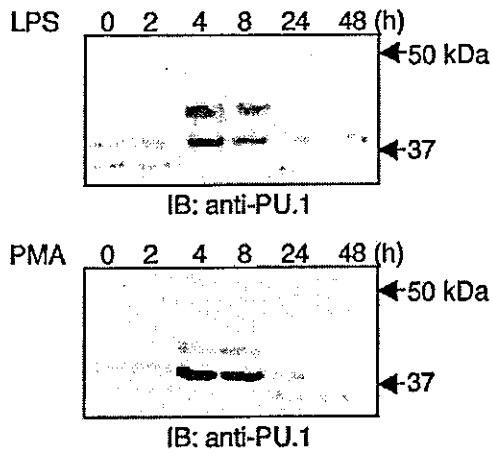

FIGURE 8. Up-regulation of endogenous PU.1 in mast cells by LPS or PMA stimulation. BMMC was incubated in culture medium in the presence of LPS (1 μg/ml) or PMA (100 mg/ml). Whole cells (1×10^6) were applied onto SDS-PAGE after 0- to 48-h incubation, as indicated at the *top* of each lane.

Fukuyama and T. Tokura for technical support, and M. Matsumoto and E. Kawasaki for secretarial assistance. We are grateful to Dr. W. Ng for proofing this manuscript.

References

1. Lloberas, J., C. Soler, and A. Celara. 1999. The key role of PU.1/SPI-1 in B cells, myeloid cells and macrophages. *Immunol. Today 20:184.*
2. McKercher, S. R., B. E. Torbett, K. L. Anderson, G. W. Henkel, D. J. Vestal, H. Baribault, M. Klemsz, A. J. Feeney, G. E. Wu, C. J. Paige, and R. A. Maki. 1996. Targeted disruption of the PU.1 gene results in multiple hematopoietic abnormalities. *EMBO J. 15:5647.*
3. Scott, E. W., M. C. Simon, J. Anastasi, and H. Singh. 1994. Requirement of transcription factor PU.1 in the development of multiple hematopoietic lineages. *Science 265:1573.*
4. Scott, E. W., R. C. Fisher, M. C. Olson, E. W. Kehrli, M. C. Simon, and H. Singh. 1997. PU.1 functions in a cell-automomous manner to control the differentiation of multipotential lymphoid-myeloid progenitors. *Immunity 6:437.*
5. Anderson, K. L., H. Perkin, C. D. Surh, S. Venturini, R. A. Maki, and B. E. Torbett. 2000. Transcription factor PU.1 is necessary for development of thymic and myeloid progenitor-derived dendritic cells. *J. Immunol. 164:1855.*
6. Guerriero, A., P. B. Langmuir, L. M. Spain, and E. W. Scott. 2000. PU.1 is required for myeloid-derived but not lymphoid-derived dendritic cells. *Blood 95:879.*
7. Walsh, J. C., R. P. DeKoter, H.-J. Lee, E. D. Smith, D. W. Lancki, M. F. Gurish, D. S. Friend, R. L. Stevens, J. Anastasi, and H. Singh. 2002. Cooperative and antagonistic interplay between PU.1 and GATA-2 in the specification of myeloid cell fates. *Immunity 17:665.*
8. DeKoter, R. P., and H. Singh. 2000. Regulation of B lymphocyte and macrophage development by graded expression of PU.1. *Science 288:1439.*
9. Dahl, R., J. C. Walsh, D. Lancki, P. Laslo, S. R. Iyer, H. Singh, and M. C. Simon. 2003. Regulation of macrophages and neutrophil cell fates by the PU.1:C/EBPα ratio and granulocyte colony-stimulating factor. *Nat. Immunol. 4:1029.*
10. Iwama, A., M. Osawa, R. Hirasawa, N. Uchiyama, S. Kaneko, M. Onodera, K. Shibuya, A. Shibuya, C. Vinson, D. G. Tenen, and H. Nakauchi. 2002. Reciprocal roles for CCAAT/enhancer binding protein (C/EBP) and PU.1 transcription factors in Langerhans cell commitment. *J. Exp. Med. 195:547.*
11. Reddy, V. A., A. Iwama, G. Iotzova, M. Schulz, A. Elsasser, R. K. Vangala, D. G. Tenen, W. Hiddemann, and G. Behre. 2002. Granulocyte inducer C/EBPα inactivates the myeloid master regulator PU.1: possible role in lineage commitment decisions. *Blood 100:483.*
12. Nishiyama, C., M. Nishiyama, T. Ito, S. Masaki, K. Maeda, N. Masuoka, H. Yamane, T. Kitamura, H. Ogawa, and K. Okumura. 2004. Overproduction of PU.1 in mast cell progenitors: its effect on monocyte- and mast cell-specific gene expression. *Biochem. Biophys. Res. Commun. 313:516.*
13. Morita, S., T. Kojima, and T. Kitamura. 2000. Plat-E: an effieicnt and stable system for transient packaging of retroviruses. *Gene Ther. 7:1063.*
14. Nakahata, T., S. S. Spicer, J. R. Cantey, and M. Ogawa. 1982. Clonal assay of mouse mast cell colonies in methylcellulose culture. *Blood 60:352.*
15. Yurt, R. W., R. W. Leid, Jr., and K. F. Austen. 1977. Native heparin from rat peritoneal mast cells. *J. Biol. Chem. 252:518.*
16. Inaba, K., M. Inaba, N. Romani, H. Aya, M. Deguchi, S. Ikehara, S. Muramatsu, and R. M. Steinman. 1992. Generation of large numbers of dendritic cells from mouse bone marrow cultures supplemented with granulocyte/macrophage colony-stimulating factor. *J. Exp. Med. 176:1693.*
17. Labeur, M. S., B. Roters, B. Pers, A. Mehling, T. A. Luger, T. Schwarz, and S. Grabbe. 1999. Generation of tumor immunity by bone marrow-derived dendritic cells correlates with dendritic cell maturation stage. *J. Immunol. 162:168.*
18. Yamazaki, T., H. Akiba, H. Iwai, H. Matsuda, M. Aoki, Y. Tanno, T. Shin, H. Tsuchiya, D. M. Pardoll, K. Okumura, et al. 2002. Expression of programmed death 1 ligands by murine T cells and APC. *J. Immunol. 169:5538.*
19. Onishi, M., S. Konoshita, Y. Morikawa, A. Shibuya, J. Phillips, L. L. Lanier, D. M. Gorman, G. P. Nolan, A. Miyajima, and T. Kitamura. 1996. Applications of retrovirus-mediated expression cloning. *Exp. Hematol. 24:324.*
20. Nishiyama, C., M. Nishiyama, T. Ito, S. Masaki, N. Masuoka, H. Yamane, T. Kitamura, H. Ogawa, and K. Okumura. 2004. Functional analysis of PU.1 domains in monocyte-specific gene regulation. *FEBS Lett. 561:63.*
21. Nishiyama, C., N. Masuoka, M. Nishiyama, T. Ito, H. Yamane, K. Okumura, and H. Ogawa. 2004. Evidence against requirement of Ser41 and Ser45 for function of PU.1: molecular cloning of rat PU.1. *FEBS Lett. 572:57.*
22. Nosaka, T., T. Kawashima, K. Misawa, K. Ikuta, A. L.-F. Mui, and T. Kitamura. 1998. STAT5 as a molecular regulator of proliferation, differentiation and apoptosis in hematopoietic cells. *EMBO J. 18:4754.*
23. Hasegawa, M., C. Nishiyama, M. Nishiyama, Y. Akizawa, K. Takahashi, T. Ito, S. Furukawa, C. Ra, K. Okumura, and H. Ogawa. 2003. Regulation of the human FcϵRI α-chain distal promoter. *J. Immunol. 170:3732.*
24. Nishiyama, C., Y. Akizawa, M. Nishiyama, T. Tokura, H. Kawada, K. Mitsuishi, M. Hasegawa, T. Ito, N. Nakano, A. Okamoto, et al. 2004. Polymorphisms in the *FcϵRIβ* promoter region affecting transcription activity: a possible promoter-dependent mechanism for association between *FcϵRIβ* and atopy. *J. Immunol. 173:6458.*
25. Furumoto, Y., S. Hiraoka, K. Kawamoto, S. Masaki, T. Kitamura, K. Okumura, and C. Ra. 2000. Polymorphisms in FcϵRI β chain do not affect IgE-mediated mast cell activation. *Biochem. Biophys. Res. Commun. 273:765.*
26. Kaisho, T., and S. Akira. 2001. Dendritic-cell function in Toll-like receptor- and MyD88-knock out mice. *Trends Immunol. 22:78.*
27. Supajatura, V., H. Ushio, A. Nakao, K. Okumura, C. Ra, and H. Ogawa. 2001. Protective roles of mast cells against enterobacterial infection are mediated by Toll-like receptor 4. *J. Immunol. 167:2250.*
28. Rehli, M., A. Poltorak, L. Schwarzfischer, S. W. Krause, R. Andreesen, and B. Beutler. 2000. PU.1 and interferon consensus sequence-binding protein regulate the myeloid expression of the human Toll-like receptor 4 gene. *J. Biol. Chem. 275:9773.*
29. Haehnel, V., L. Schwarzfischer, M. J. Fenton, and M. Rehli. 2002. Transcriptional regulation of the human *Toll-like receptor 2* gene in monocytes and macrophages. *J. Immunol. 168:5629.*
30. Katoh, N., S. Kraft, J. H. Wessendorf, and T. Bieber. 2000. The high-affinity IgE receptor (FceRI) blocks apoptosis in normal human monocytes. *J. Clin. Invest. 105:183.*
31. Chen, H. M., D. Ray-Gallet, P. Zhang, C. J. Hetherington, D. A. Gonzalez, D.-E. Zhang, F. Moreau-Gachelin, and D. G. Tenen. 1995. PU.1 (Spi-1) autoregulates its expression in myeloid cells. *Oncogene 11:1549.*
32. Lodie, T. A., J. Ricardo Savedra, D. T. Golenbock, C. P. V. Beveren, R. A. Maki, and M. J. Fenton. 1997. Stimulation of macrophages by lipopolysaccharide alters the phosphorylation state, conformation, and function of PU.1 via activation of casein kinase II. *J. Immunol. 158:1848.*
33. Carey, J. O., K. J. Posekany, J. E. deVente, G. R. Pettit, and D. K. Ways. 1996. Phorbol ester-stimulated phosphorylation of PU.1: association with leukemic cell growth inhibition. *Blood 87:4316.*
34. Rekhtman, N., F. Radparvar, T. Evans, and A. I. Skoultchi. 1999. Direct interaction of hematopoietic transcription factors PU.1 and GATA-1: functional antagonism in erythroid cells. *Genes Dev. 13:1398.*
35. Voso, M. T., T. C. Burn, G. Wulf, B. Lim, G. Leone, and D. G. Tenen. 1994. Inhibition of hematopoiesis by competitive binding of transcription factor PU.1. *Proc. Natl. Acad. Sci. USA 91:7932.*
36. Nerlov, C., and T. Graf. 1998. PU.1 induces myeloid lineage commitment in multipotent hematopoietic progenitors. *Genes Dev. 12:2403.*
37. Nishiyama, C., M. Hasegawa, M. Nishiyama, K. Takahashi, Y. Akizawa, T. Yokota, K. Okumura, H. Ogawa, and C. Ra. 2002. Regulation of human FcϵRI α-chain gene expression by multiple transcription factors. *J. Immunol. 168:4546.*
38. Maeda, K., C. Nishiyama, T. Tokura, Y. Akizawa, M. Nishiyama, H. Ogawa, K. Okumura, and C. Ra. 2003. Regulation of cell type-specific mouse FcϵRI β-chain gene expression by GATA-1 via four GATA motifs in the promoter. *J. Immunol. 170:334.*
39. Henkel, G., and M. A. Brown. 1994. PU.1 and GATA: components of a mast cell-specific interleukin 4 intronic enhancer. *Proc. Natl. Acad. Sci. USA 91:7737.*
40. Kraft, S., J. H. M. Weβendorf, D. Hanau, and T. Bieber. 1998. Regulation of the high affinity receptor for IgE on human epidermal Langerhans cells. *J. Immunol. 161:1000.*
41. Kraft, S., and T. Bieber. 2001. FcϵRI-mediated activation of transcription factors in antigen-presenting cells. *Int. Arch. Allergy Immunol. 125:9.*
42. Clark, S. C., and R. Kamen. 1987. The human hematopoietic colony-stimulating factors. *Science 236:1229.*
43. Kim, J., and R. A. Feldman. 2002. Activated Fes protein tyrosine kinase induces terminal macrophage differentiation of myeloid progenitors (U937 cells) and activation of the transcription factor PU.1. *Mol. Cell. Biol. 22:1903.*
44. Hohaus, S., M. S. Petrovick, M. T. Voso, Z. Sun, Dong-Zhang, and D. G. Tenen. 1995. PU.1 (Spi-1) and C/EBPα regulate expression of the granulocyte-macrophage colony-stimulating factor receptor α gene. *Mol. Cell. Biol. 15:5830.*
45. Zhang, D. E., C. J. Hetherington, H. M. Chen, and D. G. Tenen. 1994. The macrophage transcription factor PU.1 directs tissue-specific expression of the macrophage colony-stimulating factor receptor. *Mol. Cell. Biol. 14:373.*
46. Shibata, Y., P.-Y. Berclaz, Z. C. Chroneos, M. Yoshida, J. A. Whitsett, and B. C. Trapnell. 2001. GM-CSF regulates alveolar macrophage differentiation and innate immunity in the lung through PU.1. *Immunity 15:557.*

Kidney International, Vol. 66 (2004), pp. 597–604

Smad3 deficiency attenuates renal fibrosis, inflammation, and apoptosis after unilateral ureteral obstruction

KUMI INAZAKI, YUTAKA KANAMARU, YUKO KOJIMA, NORIYOSHI SUEYOSHI, KO OKUMURA, KAZUNARI KANEKO, YUICHIRO YAMASHIRO, HIDEOKI OGAWA, and ATSUHITO NAKAO

Atopy (Allergy) Research Center, Juntendo University School of Medicine, Tokyo, Japan; Department of Pediatrics, Juntendo University School of Medicine, Tokyo, Japan; Division of Pathology, Central Laboratory of Medical Sciences, Juntendo University School of Medicine, Tokyo, Japan; and Department of Immunology, Faculty of Medicine, University of Yamanashi, Yamanashi, Japan

Smad3 deficiency attenuates renal fibrosis, inflammation, and apoptosis after unilateral ureteral obstruction.

Background. Transforming growth factor-β (TGF-β) has been implicated in the development of renal fibrosis induced by unilateral ureteral obstruction (UUO). However, there is little information on signaling pathways mediating TGF-β activity involved in molecular and cellular events leading to renal fibrosis induced by UUO. In this study, we sought to determine whether Smad3, a major signaling component of TGF-β, mediated renal fibrosis induced by UUO.

Methods. Renal fibrosis, inflammation, and apoptosis induced by UUO were macroscopically and histologically compared between wild-type mice and Smad3 null mice.

Results. Gross appearance of the kidney after UUO showed relatively intact kidney in Smad3 null mice [Smad3(−/−) mice] when compared with that of wild-type mice [Smad3(+/+) mice]. Renal interstitial fibrosis based on the interstitial area stained with Aniline-blue or Sirius red solution was significantly attenuated in the obstructed kidney of Smad3(−/−) mice when compared with that of Smad3(+/+) mice. Deposition of type I and type III collagens were also significantly reduced in the obstructed kidney of Smad3(−/−) mice. In addition, the numbers of myofibroblasts, macrophages, and CD4/CD8 T cells infiltrated into the kidney after UUO were significantly attenuated in the obstructed kidney of Smad3(−/−) mice when compared with that of Smad3(+/+) mice. Furthermore, terminal deoxynucleotidyltransferase-mediated deoxyuridine triphosphate (dUTP) nick-end labeling (TUNEL) staining after UUO showed significantly reduced number of tubular apoptotic cells in the obstructed kidney of Smad3(−/−) mice when compared with that of Smad3(+/+) mice. Endogenous Smad pathway was activated in the obstructed kidney after UUO in wild-type mice as judged by the increase of phosphorylated Smad2 or phosphorylated Smad2/3-positive cells in renal interstitial area.

Conclusion. Smad3 deficiency attenuated renal fibrosis, inflammation, and apoptosis after UUO, suggesting that Smad3 was a key molecule mediating TGF-β activity leading to real fibrosis after UUO.

Key words: Smad, UUO, fibrosis, inflammation, apoptosis.

Received for publication August 4, 2003
and in revised form January 28, 2004, and March 1, 2004
Accepted for publication March 19, 2004

Fibrosis of the tubulointerstitial compartment often accompanied by inflammation is a major factor in progressive loss of renal function in patients with a variety of kidney diseases [1, 2]. Unilateral ureteral obstruction (UUO) is a representative model of tubulointerstitial renal fibrosis that have many readily quantifiable cellular and molecular events during the initiation and progression of renal fibrosis such as inflammation and apoptosis [3]. Although many factors are involved in the pathophysiology of UUO [3], it is well accepted that transforming growth factor-β (TGF-β) is a key molecule for the development of tubulointerstitial fibrosis in UUO [3–10]. It is generally thought that TGF-β is involved in tissue fibrosis including renal fibrosis induced by UUO based on its capacity to induce extracellular matrix (ECM) production, differentiation from fibroblasts into myofibroblasts, and apoptosis [3, 8, 11–13]. However, there is little information on signaling pathways mediating TGF-β activity that leads to renal fibrosis induced by UUO.

Although TGF-β activates multiple intracellular signaling pathways, recent intense investigations have revealed that Smad proteins constitute the basic components of the core intracellular signaling cascade carrying TGF-β signals from the cell surface directly to the nucleus [14–16]. The activated TGF-β receptors phosphorylate Smad2 and Smad3, which form heterotrimeric complex with Smad4, respectively, and enter the nucleus, bind directly or indirectly to DNA, and regulate transcription of many TGF-β target genes in cooperation with various transcriptional factors and coactivators/corepressors. Respective role of Smad2 and Smad3 in TGF-β signaling remains obscure, but reports on Smad2- and Smad3-deficient mice suggest a distinct role of Smad2 and Smad3 in vivo. Smad3 null mutant mice have been generated in

different laboratories [17–19], which were viable and fertile, in contrast to Smad2 null mice that show early embryonic lethality [20–22]. So far, the in vivo role of Smads in renal fibrosis has not been addressed.

In this study, we determined whether Smad3 played a role in the development of renal fibrosis in UUO by using Smad3-deficinet mice. We found that Smad3 deficiency attenuated renal fibrosis, inflammation, and apoptosis after UUO. Our findings suggest that Smad3 is a key molecule for cellular and molecular events involved in UUO and may thus become a novel therapeutic target for renal fibrosis.

METHODS

Mice

The generation of Smad3^{delEx8} null mice [Smad3(−/−) mice] by homologous recombination was described previously [17] and kindly provided by C. Deng (National Institutes of Health, Bethesda, MD, USA). In this line of mice, exon 8 of the Smad3 gene is deleted. The deletion removes the L3 loop, which is necessary for interaction with the TGF-β receptors, and the COOH-terminal serine-serine-valine-serine (SSVS) consensus phosphorylation site. Smad3(−/−) mice were backcrossed for six generations to C57BL6 mice as previously described [23]. Mice heterozygous for the targeted disruption were intercrossed to produce homozygous offspring and kept under specific pathogen-free conditions in the animal facility of Juntendo University.

Experimental design

Left kidney UUO was performed in male wild-type Smad3(+/+) mice and Smad3(−/−) mice, 10 to 12 weeks of age (N = 6 per group), as previously described [24]. Briefly, under anesthesia with pentobarbital sodium (0.3mg/g), UUO was created by complete double ligation of the left ureter with 2-0 silk suture through an abdominal midline incision. The mice were killed 14 days after UUO and the obstructed or intact right kidney was immediately weighed, and were fixed in 20% formalin and embedded in paraffin. Some portions of the kidney were immediately frozen in Tissue-Tek 22-oxacalcitriol (OCT) compound for immunohistochemical analysis. All animal experiments were performed according to the approved manual of the Institutional Review Board of Juntendo University. Preliminary studies confirmed that there were little renal fibrosis, inflammation, and apoptosis in sham-operated left kidney of Smad3(+/+) and Smad3(−/−) mice 14 days after the operation.

Histologic examination

The kidney sections (4 μm-thick) were stained with hematoxylin and eosin, periodic acid-Schiff, Aniline-blue, or Sirius red solutions. The severity of interstitial renal fibrosis was evaluated by the calculation of the positive area of Aniline-blue or Sirius red staining of one slide section measured with a computerized image analyzer (KS400) (Carl Zeiss Vision GmbH, Hallbergmoos, Germany).

Immunohistochemical staining

Interstitial cellularity or collagen deposition was characterized and quantified after immunoperoxidase staining for macrophages with F4/80 rat antimouse macrophage monoclonal antibody (Serotec Ltd., Oxford, UK), for myofibroblasts with peroxidase-conjugated murine antihuman α-smooth muscle actin (α-SMA) 1A4 monoclonal antibody (Dako Corp., Carpinteria, CA, USA), for T cells with rat antimouse CD4 and CD8 antibodies (BD Pharmingen, San Diego, CA, USA), and for collagens with antibodies against type I or type III collagen (Southern Biotechnology, Birmingham, AL, USA). Phosphorylated Smad2 or Smad2/3 expression in renal tissue was immunohistochemically detected by using antibodies against phosphorylated Smad2 (Cell Signaling Technology Inc., Beverly, MA, USA) or antiphosphorylated Smad2/3 (Santa Cruz Biotechnology, Santa Cruz, CA, USA). Sections with secondary antibody alone were negative. Scoring of F4/80-postive cells was determined to be 0, <5% of positive area in one high power field (×400); 1, 5% to 25% of positive area; 2, 25% to 50% of positive area; and 3, 50% to 75% of positive area; and 4, >75% of positive area. Random six high power fields were selected and scored. The number of CD4 or CD8-positive interstitial cells was counted manually in six random high power fields. α-SMA–positive area was measured with a computerized image analyzer (KS400) (Carl Zeiss Vision GmbH) as described above.

TUNEL assay

In situ detection of DNA fragmentation was performed using terminal deoxynucleotidyltransferase-mediated deoxyuridine triphosphate (dUTP) nick-end labeling (TUNEL) staining using in situ tunnel staining kit (Takara Bio, Inc., Ohtsu, Shiga, Japan) according to the manufacturer's recommendation. The number of TUNEL-positive cells was counted in six random high power fields.

Data analysis

Statistical analysis was performed using an unpaired the Student t test. Data were shown as mean ± SD and $P < 0.05$ was considered to be significant.

RESULTS

Phenotype of Smad3 null mice

A significant fraction (~50%) of Smad3(−/−) mice kept in our specific pathogen-free facility developed a

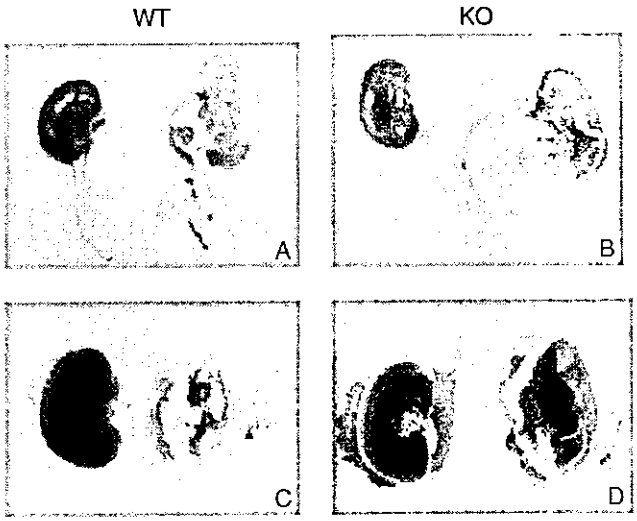

Fig. 1. Gross appearance of the mouse kidney 14 days after unilateral ureteral obstruction (UUO). The left obstructed kidney or right nonobstructed kidney of Smad3(+/+) and Smad3(−/−) mice were removed 14 days after UUO. Representative pictures of the kidneys from Smad3(+/+) mice (*A* and *C*) and from Smad3(−/−) mice (*B* and *D*) were shown. (C and D) Cross-section of the left and right kidneys. Note that the obstructed kidney of Smad3(−/−) mice showed relatively intact kidney tissue (much less whitish scar area than that of Smad3(+/+) mice). Abbreviations are: WT, wild-type; KO, knockout.

wasting syndrome associated with impaired mucosal immunity and abscess formation, and died between 1 and 4 months of age as previously described [17]. Yang et al [17] described that Smad3(−/−) mice exhibited reduced size compared with their littermate controls and developed bacterial abscesses near eyes, mandible, salivary glands, and intestine. This phenotype could be attributed, at least in part, to impaired chemotactic response of neutrophils toward TGF-β because the presence of neutrophils within the abscesses was few [17]. These mice were not used for the analysis. However, the remaining Smad3(−/−) mice appeared to develop normally, although slightly smaller than their littermates, and lived for at least 4 to 8 months. The kidneys of these mice were histologically intact and serum blood urea nitrogen (BUN) and creatinine levels were normal at the age of 10 to 12 weeks (data not shown). Thus, we decided to use these mice for the following studies and matched the Smad3(−/−) mice for weight as closely as possible with their wild-type controls.

Renal fibrosis

To determine whether Smad3 deficiency affected renal fibrosis in vivo, the severity of renal fibrosis and inflammation caused by UUO was compared in Smad3 wild-type (+/+) and Smad3-deficient (−/−) mice. Smad3(+/+) and Smad3(−/−) mice that underwent UUO were sacrificed for evaluation of renal lesion 14 days after UUO. As shown in Figure 1, gross appearance showed remarkable

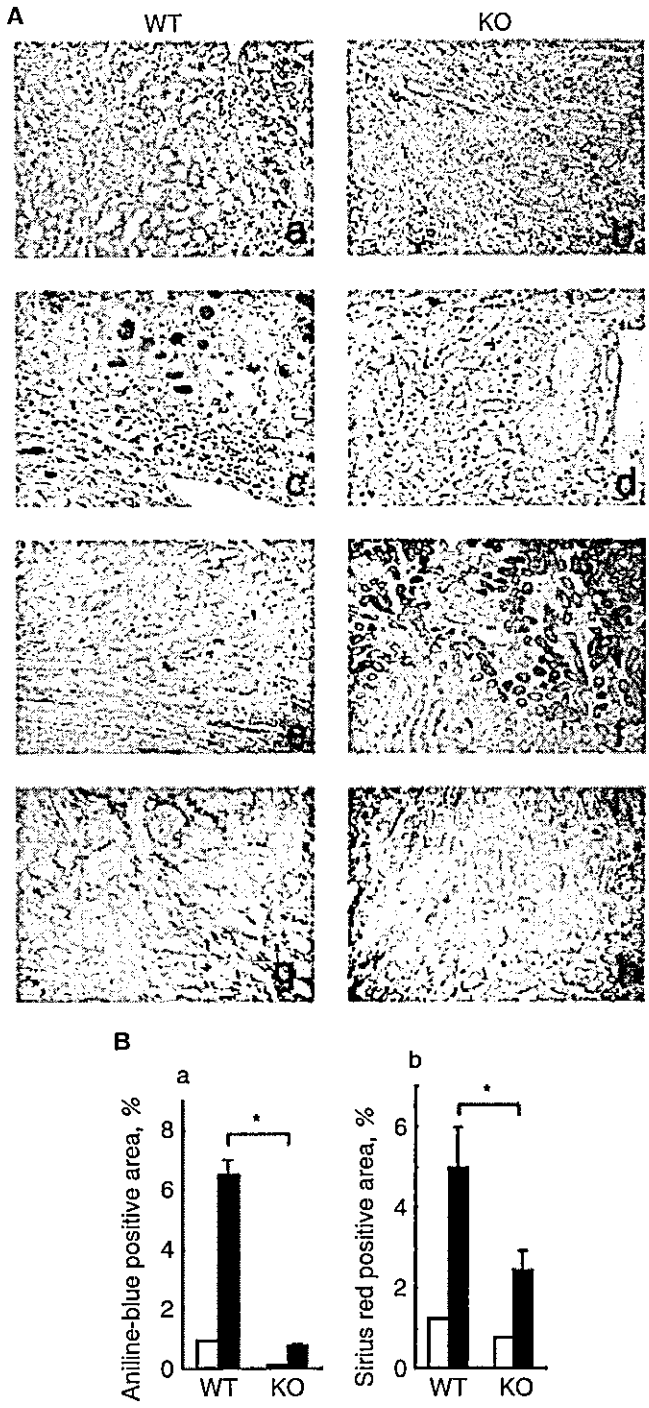

Fig. 2. Renal histology of the obstructed kidney after unilateral ureteral obstruction (UUO). (*A*) The left obstructed kidney were removed from Smad3(+/+) and Smad3(−/−) mice 14 days after UUO and the kidney sections were prepared and stained with hematoxylin-eosin (a and b), periodic acid-Schiff (c and d), Aniline-blue (e and f), or Sirius red (g and h) solutions. Representative pictures of the kidneys from Smad3(+/+) mice (a, c, e, and g) and from Smad3(−/−) mice (b, d, f, and h) are shown. (*B*) Quantitative analysis of Aniline-blue or Sirius red staining. The Aniline-blue (a) or Sirius-red (b) positive area of one slide of the left obstructed (■) or nonobstructed right kidney (□) of Smad3(+/+) mice [wild-type (WT)] and Smad3(−/−) mice [knockout (KO)] 14 days after UUO was measured with a computerized image analyzer as described in the **Methods** section. Results were expressed as percentage of positive area of one slide ($N = 6$). $^*P < 0.05$.

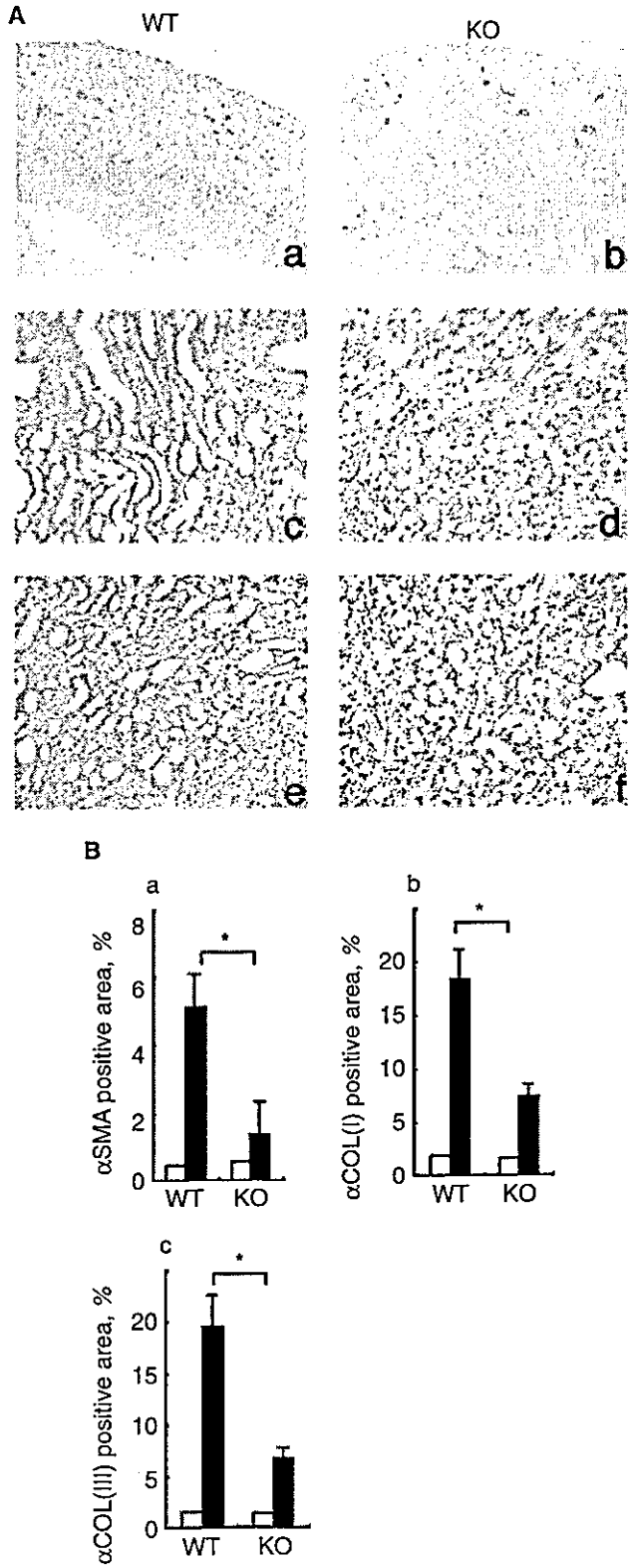

Fig. 3. Reduced number of α-smooth muscle actin (α-SMA)–positive cells or deposition of type I and type III collagens in the obstructed kidney of Smad3(−/−) mice after unilateral ureteral obstruction (UUO). (*A*) Representative pictures showing immunohistochemical staining with anti-α−SMA (a and b), anti-type I collagen (c and d), or anti-type III collagen (e and f) antibody of the kidney sections from Smad3(+/+) mice [wild-type (WT) left panels] and Smad3(−/−) mice [knockout (KO) right panels] 14 days after UUO. (*B*) Quantitative analysis of α-SMA, type I collagen, or type III collagen positive areas. The α-SMA (a), type I collagen (b), or type III collagen (c) positive area of one slide of the left obstructed (■) or nonobstructed right kidney (□) of Smad3(+/+) mice (WT) and Smad3(−/−) mice (KO) 14 days after UUO was measured with a computerized image analyzer as described in the **Methods** section. The results were expressed as percentage of positive area of one slide ($N = 6$). $^*P < 0.05$.

reduction of scar formation (whitish area in the kidney) in the obstructed kidney of Smad3(−/−) mice after UUO when compared with that of Smad3(+/+) mice. Interestingly, the size of hydronephrosis was bigger in Smad3(−/−) mice than that of Smad3(+/+) mice, suggesting that urine secretion/absorption (or renal function) was relatively maintained in Smad3(−/−) mice. Indeed, there was significant difference in the urine volume deposited in hydronephrosis between Smad3(+/+) mice and Smad3 (−/−) mice [urine volume Smad3(+/+) mice 196.7 ± 32.3 μL versus Smad3(−/−) mice 591.7 ± 149.1 μL, $P = 0.03$, $N = 6$]. Histologically, quantitative analysis of Aniline-blue or Sirius red staining after UUO revealed that the obstructed kidney of Smad3(−/−) mice had significantly reduced the staining intensity when compared with that of Smad3(+/+) mice (Fig. 2B).

It is now clear that myofibroblasts, a subpopulation of specialized fibroblasts which express the smooth muscle isoform of α-actin (α-SMA), play a central role in the mediation of tissue fibrosis with their augmented ability to produce ECM and contraction [13]. The number of interstitial myofibroblasts (α-SMA–positive cells) was increased in the obstructed kidney of Smad3(+/+) mice after UUO as previously described [23], but the intensity of the response was significantly attenuated in the obstructed kidney of Smad3(−/−) mice (Fig. 3). In addition, deposition of type I and type III collagens were significantly decreased in the obstructed kidney of Smad3(−/−) mice (Fig. 3)

Renal inflammation

Hematoxylin-eosin staining of the kidney sections suggested reduced inflammation after UUO in the obstructed kidney of Smad3(−/−) mice when compared with that of Smad3(+/+) mice (Fig. 2). The finding was supported by quantitative analysis of the number of F4/80-positive interstitial macrophages, CD4-postive T cells, and CD8-positive T cells showing reduced number of these inflammatory cells in the obstructed kidney of Smad3(−/−) mice when compared with that of Smad3(+/+) mice (Fig. 4).

Renal apoptosis

To determine renal tubular apoptosis after UUO, the TUNEL assay was performed in paraffin-embedded